

SCATTERING IN QUANTUM ELECTRODYNAMICS
AT INFINITE MOMENTUM AND THE REGGE-EIKONAL APPROXIMATION†

John B. Kogut*

Stanford Linear Accelerator Center
Stanford University, Stanford, California 94305

ABSTRACT

We discuss the Regge-eikonal calculational scheme within the context of quantum electrodynamics in the infinite momentum frame. Our formulation of high energy scattering enjoys a simple physical picture which is a realization of Feynman's parton ideas. Armed with this clear physical picture, we derive the popular Regge-eikonal scattering amplitude, and clarify the assumptions underlying this model. Our calculational scheme suggests the presence of certain diagrams which are not included in the Regge-eikonal approximation. We present a detailed model calculation of a class of such graphs and find, on the basis of their rapid growth with energy, that they should not be ignored in a realistic calculation. We are led to conclude that the Regge-eikonal scheme does not provide a physically compelling picture of diffraction scattering.

†Work supported by the U.S. Atomic Energy Commission

*NSF Predoctoral Fellow

I. INTRODUCTION

Numerous authors, led in particular by H. Cheng and T. T. Wu,¹ have recently been attempting to understand the diffractive aspects of high energy strong interaction scattering amplitudes by studying field theory. The motivation for undertaking such a prodigious project is the fact that field theory, as opposed to other models of strong interactions, respects the cherished principles of crossing, unitarity, and analyticity. However, since perturbation theory is the only calculational technique at ones disposal, it is difficult to see how one can obtain predictions from field theory which do not rely on the unrealistic assumption of weak coupling. One particular way out has been, of course, to sum infinite sets of Feynman diagrams. This procedure is, in general, mathematically unjustifiable but has been used with some apparent success recently in discussing the high energy limits of elastic and inelastic cross sections.

In two previous articles² (to be referred to as I and II), this author, in collaboration with J. D. Bjorken and D. E. Soper, has developed an approach to these problems which seems particularly convenient and physical. In I we reformulated QED in an infinite momentum frame. Although this theory was shown to be formally equivalent to QED formulated in a realizable reference frame, it possessed certain calculational and conceptual simplifications which suggested that it would provide a useful framework for discussing high energy scattering processes. This program was begun in II where we considered the scattering of energetic electrons and photons off an external field and found that a physical picture emerged which provided a concrete example of Feynman's "parton" ideas.³ In more detail, we found that a very high energy scattering process can be viewed in three steps: the incoming physical particle dissociates into a

long lived intermediate state of bare constituents; these constituents (quanta of the Schroedinger fields) interact with the external field and pick up eikonal phases; and finally, these constituents interact among themselves and compose a certain final physical state. Using the very convenient calculational techniques of QED at infinite momentum, we were able to obtain the high energy limits of many electrodynamic scattering amplitudes.

In this paper we wish to continue the considerations of II. To begin, we will complete our study of multiperipheral chains (Fig. 7). Some of these calculations have appeared in the literature so the details of this work will be relegated to several lengthy appendices. We will, however, verify that the scattering amplitude given by the sum of single chain diagrams is a branch cut extending to the right of $J = 1$ and so violates the Froissart bound. It has been suggested⁴ that s-channel unitarity be restored by iterating the multiperipheral chain. We will see that our parton picture leads to such effects in a natural and physically lucid fashion. However, our physical picture also suggests that it may not be reasonable to treat multiperipheral chains as non-interfering, non-interacting units as has been done in the current Regge-eikonal calculations. In order to strengthen this claim, we calculate a class of diagrams which lie outside the Regge-eikonal scheme and find that their energy dependence exceeds the energy dependence of the single chain graphs. Although these calculations are done in a simpler model than QED, it is argued that they possess enough of the decisive elements of the true QED problem to be indicative of the truth. On the basis of these arguments we are led to speculate that diagrams involving several several multiperipheral chains which interfere and interact with one another play an important role in diffraction scattering.

II. CALCULATIONAL TECHNIQUES

QED at infinite momentum has been developed and applied in I and II. The reader is referred to I and Section II of II for a detailed account of the canonical field theory at infinite momentum. We will, however, summarize those features of the formalism which will be used in the calculations here.

Recall that it is the τ -evolution operator, $U(\tau', \tau)$, which plays the central role in the calculational procedure and physical picture. It is defined by,

$$U(\tau', \tau) = \exp(i h_0 \tau') \exp\left(-i [h_0 + h_I] [\tau' - \tau]\right) \exp(-i h_0 \tau) \quad (\text{II. 1})$$

where h_0 is the free particle infinite momentum Hamiltonian and $h_0 + h_I$ is the full infinite momentum Hamiltonian for QED with no external field present. The operator $U(0, -\infty)$ relates a bare (eigenstate of h_0) state, $|a\rangle$, labelled with quantum numbers 'a', to a physical (eigenstate of $h_0 + h_I$) state, $|i(a)\rangle$, by

$$|i(a)\rangle = U(0, -\infty) |a\rangle \quad (\text{II. 2})$$

A final physical state $|f(b)\rangle$ is then related to the corresponding bare particle state $|b\rangle$ by $|f(b)\rangle = U(0, \infty)|b\rangle$. We have shown in II that the S matrix describing scattering of high energy particles off an external field $a_\mu(x)$ is then simply,

$$\langle b|S|a\rangle = \delta_{ba} + \langle b|U(\infty, 0)(\mathbb{F} - 1)U(0, -\infty)|a\rangle \quad (\text{II. 3})$$

where \mathbb{F} is the eikonal phase operator,

$$\mathbb{F} = \exp \left\{ -i \int d\underline{x} \chi(\underline{x}) \rho(\underline{x}) \right\} \quad (\text{II. 4})$$

and,

$$\begin{aligned} \chi(\underline{x}) &= e \int d\tau a_0(\tau, \underline{x}, 0) \\ \rho(\underline{x}) &= \int d\underline{z} \psi^\dagger(0, \underline{x}, \underline{z}) \psi(0, \underline{x}, \underline{z}) \end{aligned} \quad (\text{II. 5})$$

It is (II. 3) which leads to the physical picture as described in the Introduction.

Although the formal derivation of (II. 3) does not rely upon perturbation theory, we will use perturbation theory to expand the physical states in terms of bare constituents. To this end recall the formula for the one particle state $|i(a)\rangle$,

$$\begin{aligned} |i(a)\rangle &= \sqrt{Z_a} \left\{ |a\rangle + \sum'_n |n\rangle \frac{1}{H_i - H_n} \langle n | h_I | a \rangle + \right. \\ &\quad \left. \sum'_n \sum'_m |n, h_I, m\rangle \frac{1}{H_i - H_n} \langle n, h_I, m | h_I | a \rangle + \dots \right\} \end{aligned} \quad (\text{II. 6})$$

where H_n is the infinite momentum energy of the bare state $|n\rangle$ and the sums \sum' exclude the single bare particle state $|a\rangle$. The wave function renormalization constant $\sqrt{Z_a}$ is determined by the unitarity of the τ -evolution operator,

$$\langle a | U(\infty, 0) U(0, -\infty) | a' \rangle = \langle a | a' \rangle \quad (\text{II. 7})$$

To complete the perturbative calculation of the S matrix element, we must know the effect of the eikonal phase operator on bare particles. This is easy to compute and has been done in II (Section III). Recall that bare photons are unaffected by the external potential, but electrons and positrons acquire a phase,

$$\begin{aligned} \mathbb{F} \psi^\dagger(0, \underline{x}, \underline{z}) \mathbb{F}^{-1} &= e^{-i\chi(\underline{x})} \psi^\dagger(0, \underline{x}, \underline{z}) \\ \mathbb{F} \psi(0, \underline{x}, \underline{z}) \mathbb{F}^{-1} &= e^{i\chi(\underline{x})} \psi(0, \underline{x}, \underline{z}) \end{aligned} \quad (\text{II. 8})$$

Thus, a typical matrix element of $(F-1)$ between states of two electrons and one positron, for example, would read,

$$\begin{aligned} < e^+ (\underline{p}'_1, \eta'_1) e^- (\underline{p}'_2, \eta'_2) e^- (\underline{p}'_3, \eta'_3) | (F-1) | e^+ (\underline{p}_1, \eta_1) e^- (\underline{p}_2, \eta_2) e^- (\underline{p}_3, \eta_3) > = \\ & [(2\pi)^2 \eta_1 \delta(\eta'_1 - \eta_1)] [(2\pi)^2 \eta_2 \delta(\eta'_2 - \eta_2)] [(2\pi)^2 \eta_3 \delta(\eta'_3 - \eta_3)] \times \\ & [F_c(\underline{p}'_1 - \underline{p}_1) F_c(\underline{p}'_2 - \underline{p}_2) F_c(\underline{p}'_3 - \underline{p}_3) - (2\pi)^6 \delta(\underline{p}'_1 - \underline{p}_1) \delta(\underline{p}'_2 - \underline{p}_2) \delta(\underline{p}'_3 - \underline{p}_3)] - \left(\begin{array}{c} \text{exchange} \\ \text{term} \end{array} \right) \end{aligned} \quad (\text{II. 9})$$

where

$$F(\underline{q}) = \int d\underline{x} e^{-i\underline{q} \cdot \underline{x}} e^{-i\chi(\underline{x})}, \quad F_c(\underline{q}) = \int d\underline{x} e^{-i\underline{q} \cdot \underline{x}} e^{+i\chi(\underline{x})} \quad (\text{II. 10})$$

Using the expansion (II. 6), (II. 3) and the properties of F , we can obtain perturbation theory rules which allow one to compute scattering amplitudes to a given order in the structure of a physical particle but to all orders in the external field. Similar rules were recorded in II, but a slightly different notation is advantageous for the goals of this paper. Using the notation of I (Section III), we associate the following factors with the parts of a certain τ -ordered diagram:

- (i) wave functions $u(\underline{p}, s)$, $\bar{u}(\underline{p}, s)$, $\bar{u}_c(\underline{p}, s)$, $u_c(\underline{p}, s)$, and $e_\lambda(\underline{p})$ for the external lines;
- (ii) $(\not{p} + m) = \sum_S u(\underline{p}, s) \bar{u}(\underline{p}, s)$ for electron propagators;
 $(-\not{p} + m) = -\sum_S u_c(\underline{p}, s) \bar{u}_c(\underline{p}, s)$ for positron propagators;
 $\sum_\lambda e_\lambda(\underline{p})^\mu e_\lambda(\underline{p})^\nu$ for photon propagators;
- (iii) $e\gamma_\mu$ for each vertex in Fig. 1a.
 $e^2 \delta_3^\mu \delta_3^\nu \frac{1}{\eta_0^2} \dots \gamma_\mu \dots \gamma_\nu \dots$ for each vertex in Fig. 1b, where η_0 is the total η transferred across the vertex
 $e^2 \gamma_\nu \gamma^0 \gamma_\mu \frac{1}{\eta_0}$ for each vertex in Fig. 1c;

- (iv) a factor $(2\pi)^3 \delta(\eta_{\text{out}} - \eta_{\text{in}}) \delta(\underline{p}_{\text{out}} - \underline{p}_{\text{in}})$ for each vertex;
- (v) a factor $(H_f - H + i\epsilon)^{-1}$ for each intermediate state;
- (vi) an integration $(2\pi)^{-3} \int d\underline{p} \int_0^\infty \frac{d\eta}{2\eta}$ and a sum over spins for each internal line;
- (vii) an eikonal phase factor for a chosen intermediate state.

III. SINGLE CHAIN

In this section we wish to emphasize some of the physical features and important formulas for the multiperipheral processes shown in Figs. 2-7. These processes have been considered in the literature,⁴ so we relegate our explicit and lengthy calculations of the associated scattering amplitudes to the Appendices. The reader is, however, advised to familiarize himself with some of the main features of these calculations before venturing on.

Our physical picture allows us to look at these scattering processes in three parts. First, the incoming physical electron dissociates into a state of bare constituents which in this case are e^+e^- pairs. The scattering amplitude receives its dominant (leading logarithm of energy) contribution from multiperipheral chains which are strongly ordered, i. e., the ratios of the longitudinal momenta of successive virtual photons down the chain are small. So, to good approximation the physical electron consists of a chain of e^+e^- pairs whose longitudinal momentum decreases the further down the chain we move. The chain of constituents next scatters off the external field when the slowest e^+e^- pair picks up eikonal phases (Fig. 7). Finally, the scattered state of constituents recombines into the outgoing physical electron.

According to (C.10) of Appendix C, the scattering amplitude (forward direction) for this process reads,

$$S^{(1 \text{ chain})}(\eta) = -(2\pi)(2\eta) \delta(\eta - \eta') \left[M(\eta/\eta_{\text{min}}) - 1 \right] \quad (\text{III. 1})$$

where

$$M(\eta/\eta_{\min}) = \frac{1}{\lambda^2} \int \frac{d\beta}{(2\pi)^2} f^*(\beta, 1) f(\beta, 1) \left(\frac{\eta}{\eta_{\min}} \right)^{\left(\frac{2\alpha}{\pi} \right)^2} \bar{C}(\beta) \theta \left(\frac{\eta}{\eta_{\min}} - 1 \right)$$

and η refers to the incident electron and the functions f and C are derived in Appendix D. The minus sign in (III.1) indicates that the scattering is pure absorption. The scattering amplitude can be understood more clearly by transforming it to the complex angular momentum plane. As discussed in Appendix C, the Mellin transform of (III.1) reads,

$$M(J) = \frac{1}{\lambda^2} \int \frac{d\beta}{(2\pi)^2} f^*(\beta, 1) f(\beta, 1) \left[\frac{1}{J - \left(\frac{2\alpha}{\pi} \right)^2 \bar{C}(\beta)} \right] \quad (\text{III. 2})$$

which possesses a cut over that range of J where the denominator, $J - \left(\frac{2\alpha}{\pi} \right)^2 \bar{C}(\beta)$, can vanish. That range is, in fact, from $J = 0$ to $J = 11\pi\alpha^2/32$. As derived in Appendix C this implies that the energy dependence of the S matrix element reads,

$$S^{(1\text{-chain})}(\eta) \sim - \frac{1 + \frac{11\pi\alpha^2}{32}}{\eta \sqrt{\log \eta}} \quad (\text{III. 3})$$

This result has been obtained by Frolov et al.,⁵ and disagrees slightly with the cut claimed by Cheng and Wu.⁴ We see that (III.3) violates the Froissart bound no matter how small α is. In effect, the multiperipheral chain has provided a mechanism whereby the two photons coming off the through-going electron line tend to attract one another. This effect elevates the energy dependence of the S matrix from η , characteristic of spin one photons, to $\eta^{1+(11\pi\alpha^2/32)}$.

It is this violation of the Froissart bound which has caused several authors to consider diagrams of iterations of the multiperipheral chains as a possible mechanism for softening the energy dependence of (III.3). The success of this scheme relies upon the observation that such diagrams have alternating signs

and hence tend to cancel when summed. This behavior is similar in character to the simpler and more familiar s-channel iteration procedures used in eikonal approximations. We will see in the next section that such g-channel iterations can be easily computed and understood from our infinite momentum point of view.

IV. TWO-CHAIN DIAGRAMS

In this section we will look in detail at the diagram in Fig. 8. The incident electron emits two photons which break up into two pairs which scatter simultaneously in the external field before they each coalesce back into photons which subsequently land on the outgoing electron. In addition to the particular τ -ordered graph drawn in Fig. 8 there is a graph for each other allowable τ -ordering of the vertices. The crucial point, however, is that although a particular τ -ordered graph is complicated, the sum of all the graphs is simple.

To see this consider Fig. 9 which shows a particular τ -ordered diagram which contributes to the incident physical electron state. Each vertical line in the figure denotes a certain intermediate state and energy denominator. In addition to just this τ -ordered diagram, there are diagrams for each of the 5 other permutations of the vertices (1234). There are two points concerning these diagrams we must make. First, to leading order in η_P , the vertices on the through-going electron line do not distinguish between the order of emission of the various photons. This is so because the η 's of all the photons are predominantly small compared to η_P , and the photons couple to the electron line through γ^0 which behaves like

$$\bar{u}(p, s) \gamma^0 u(P, S) = 2\sqrt{\eta_P \eta} \delta_{sS} \approx 2\eta_P \delta_{sS} \quad (\text{IV.1})$$

Secondly, the infinite momentum energy of the through-going electron can be ignored in the energy denominators for each diagram. Using this simplification we will write down the energy denominator factors for each diagram.

$$(1234) \quad \left\{ \omega(k) [H(p_3)+H(p_4)] [\omega(q)+H(p_3)+H(p_4)] [H(p_1)+H(p_2)+H(p_3)+H(p_4)] \right\}^{-1}$$

$$(1324) \quad \left\{ \omega(k) [\omega(k)+\omega(q)] [\omega(q)+H(p_3)+H(p_4)] [H(p_1)+H(p_2)+H(p_3)+H(p_4)] \right\}^{-1}$$

$$(3124) \quad \left\{ \omega(q) [\omega(q)+\omega(k)] [\omega(q)+H(p_3)+H(p_4)] [H(p_1)+H(p_2)+H(p_3)+H(p_4)] \right\}^{-1}$$

$$(1342) \quad \left\{ \omega(k) [\omega(k)+\omega(q)] [\omega(k)+H(p_1)+H(p_2)] [H(p_1)+H(p_2)+H(p_3)+H(p_4)] \right\}^{-1}$$

$$(3142) \quad \left\{ \omega(q) [\omega(q)+\omega(k)] [\omega(k)+H(p_1)+H(p_2)] [H(p_1)+H(p_2)+H(p_3)+H(p_4)] \right\}^{-1}$$

$$(3412) \quad \left\{ \omega(q) [H(p_1)+H(p_2)] [\omega(k)+H(p_1)+H(p_2)] [H(p_1)+H(p_2)+H(p_3)+H(p_4)] \right\}^{-1}$$

The sum is computed efficiently if we combine the first three terms, then the second three terms and sum the results to obtain,

$$\left\{ \omega(k) [H(p_3)+H(p_4)] \right\}^{-1} \left\{ \omega(q) [H(p_1)+H(p_2)] \right\}^{-1} \quad (\text{IV.3})$$

This important factorization property means that the two bare pairs in the physical state are independent of one another (in the region of phase space which gives the dominant contribution to the scattering amplitude). Using the ideas in this example, it is not difficult to construct an inductive proof of the factorization property for any strongly-ordered multi-chain graph.⁶ In fact, QED experts will recognize this factorization property as simply a slight variation on an argument familiar from bremsstrahlung and infrared problems.

We now return to Fig. 8, and write the scattering amplitude,

$$\begin{aligned}
S = & \frac{1}{2!} \frac{e^4}{(2\pi)^9} \delta(\eta_{\underline{p}} - \eta_{\underline{p}'}) \int M^{(1)}(\underline{p}' - \underline{p}; \eta) 2\eta \delta(\eta' - \eta) \\
& d\underline{p}' d\underline{k}_1 d\underline{p}_1 d\underline{p}_4 d\underline{\eta}_{\underline{k}_1} d\underline{\eta}_1 d\underline{\eta}' (2\eta)^{-2} (2\eta_{\underline{k}_1})^{-2} (2\eta_1)^{-2} (2\eta_4)^{-2} \\
& [\omega(\underline{k}_1)]^{-1} [\omega(\underline{k}_2)]^{-1} [H(\underline{p}_1) + (\underline{p}_2)]^{-1} [H(\underline{p}_3) + H(\underline{p}_4)]^{-1} \sum_{\underline{s}, \underline{s}'} \bar{u}(\underline{P}'\underline{s}') \gamma^{\underline{o}}_{\underline{u}(\underline{p}'\underline{s}')} \bar{u}(\underline{p}'\underline{s}') \gamma^{\underline{o}}_{\underline{u}(\underline{P}, \underline{s})} \\
& \text{tr} \left[(\not{\underline{p}}_1 + m) \gamma^{\underline{o}} (\not{\underline{p}}_4 + m) \gamma^{\underline{3}} (-\not{\underline{p}}_3 + m) \gamma^{\underline{o}} (-\not{\underline{p}}_2 + m) \gamma^{\underline{3}} \right] \left[F(\underline{p}_4 - \underline{p}_1) F_c(\underline{p}_3 - \underline{p}_2) - (2\pi)^2 \delta(\underline{p}_4 - \underline{p}_1) \delta(\underline{p}_3 - \underline{p}_2) \right]
\end{aligned} \tag{IV.4}$$

where

$$\begin{aligned}
\underline{k}_2 - \underline{k}_1 &= \underline{P}' - \underline{P} - \underline{p}' + \underline{p} \\
\underline{p}_2 = \underline{k}_1 - \underline{p}_1 &= \underline{P} - \underline{p} - \underline{p}_1, \quad \underline{p}_3 = \underline{k}_2 - \underline{p}_4 = \underline{P}' - \underline{p}' - \underline{p}_4
\end{aligned}$$

and where we have identified the scattering amplitude for the "inner" loop and have used (A.13). The factor of $\frac{1}{2!}$ occurs because when we sum over the permutations of the vertices we effectively double count individual diagrams. We can further simplify (IV.4) by noting that the η' integration is done by the δ function coming from the inner loop. Finally, identifying the scattering amplitude for the "outer" loop,

$$S = (2\pi) 2\eta_{\underline{p}} \delta(\eta_{\underline{p}} - \eta_{\underline{p}'}) \frac{1}{2!} \int \frac{d\underline{p}'}{(2\pi)^2} M^{(1)}(\underline{p}' - \underline{p}; \eta_{\underline{p}'}) M^{(1)}(\underline{P}' - \underline{P} - \underline{p}' + \underline{p}; \eta_{\underline{p}'}) \tag{IV.5}$$

This convolution integral can be factored by transforming to \underline{x} -space. Define,

$$M^{(1)}(\underline{q}; \eta_{\underline{p}}) = \int d\underline{x} e^{i\underline{q} \cdot \underline{x}} M^{(1)}(\underline{x}; \eta_{\underline{p}}) \tag{IV.6}$$

Then,

$$S = 2 \eta_p^{(2\pi)} \delta(\eta_p - \eta_{p'}) \int d\underline{x} e^{i(\underline{P}' - \underline{P}) \cdot \underline{x}} \frac{1}{2!} \left[M^{(1)}(\underline{x}, \eta_p) \right]^2 \quad (\text{IV. 7})$$

which shows the beginnings of the expected "eikonalization."

Using the same techniques we can obtain the scattering amplitude for the diagrams indicated in Fig. 10. The result is, using the notation of Appendix A and B,

$$S = 2 \eta_p^{(2\pi)} \delta(\eta_p - \eta_{p'}) \int \frac{d\underline{p}'}{(2\pi)^2} M^{(1)}(\underline{p}' - \underline{p}; \eta_p) M^{(2)}(\underline{P}' - \underline{P} - \underline{p}' + \underline{p}; \eta_p) \quad (\text{IV. 8})$$

$$S = 2 \eta_p^{(2\pi)} \delta(\eta_p - \eta_{p'}) \int d\underline{x} e^{i(\underline{P}' - \underline{P}) \cdot \underline{x}} M^{(1)}(\underline{x}, \eta_p) M^{(2)}(\underline{x}, \eta_p)$$

In this case, when summing over the permutations of the vertices, there is no overcounting of diagrams.

Continuing the argument to contain all two chain diagrams, as indicated in Fig. 11, we conclude that the scattering amplitude for this class of diagrams reads,

$$S^{(2 \text{ chain})} = 2 \eta_p^{(2\pi)} \delta(\eta_p - \eta_{p'}) \int d\underline{x} e^{i(\underline{P}' - \underline{P}) \cdot \underline{x}} \frac{1}{2!} \left[M^{(1)}(\underline{x}, \eta_p) + M^{(2)}(\underline{x}, \eta_p) + \dots \right] \left[M^{(1)}(\underline{x}, \eta_p) + \dots \right] \quad (\text{IV. 9})$$

Identifying $M^{(1 \text{ chain})}(\underline{x}, \eta_p)$ as in Appendix C, we have

$$S^{(2 \text{ chain})} = 2 \eta_p^{(2\pi)} \delta(\eta_p - \eta_{p'}) \int d\underline{x} e^{i(\underline{P}' - \underline{P}) \cdot \underline{x}} \frac{1}{2!} \left[M^{(1 \text{ chain})}(\underline{x}, \eta_p) \right]^2 \quad (\text{IV. 10})$$

V. THE REGGE-EIKONAL FORMULA - A CRITICISM

The arguments presented in the previous section generalize straightforwardly to diagrams which contain N chains scattering off an external field. Again, after summing over all τ -ordered diagrams, the chains become independent (in that region of phase space which contributes the leading log to the scattering amplitude), and the amplitude reads,

$$S^{(N)}(\underline{P}' - \underline{P}) = 2 \eta_P (2\pi) \delta(\eta_P - \eta_{P'}) \int d\underline{x} e^{i(\underline{P}' - \underline{P}) \cdot \underline{x}} \frac{1}{N!} \left[M^{(1 \text{ chain})}(\underline{x}, \eta_P) \right]^N \quad (\text{V. 1})$$

Summing over N , we find

$$S(\underline{P}' - \underline{P}) = -2 \eta_P (2\pi) \delta(\eta_P - \eta_{P'}) \int d\underline{x} e^{i(\underline{P}' - \underline{P}) \cdot \underline{x}} \left[1 - e^{-M^{(1 \text{ chain})}(\underline{x}, \eta_P)} \right] \quad (\text{V. 2})$$

which is the Regge-eikonal form for the scattering amplitude.

(V. 2) has been investigated in detail for QED and $\lambda \phi^3$ field theories.⁷

The calculation for $\lambda \phi^3$ is particularly simple, and using the techniques of this paper or otherwise, it is easy to find that,

$$M^{(1 \text{ chain})}(\underline{x}, \eta_P) \sim - \frac{\eta_P^{\alpha(0)-1}}{\log \eta_P} e^{-\frac{\underline{x}^2}{2|\alpha'(0)| \log \eta_P}} \quad (\text{V. 3})$$

where $\alpha(0)$ and $\alpha'(0)$ are, respectively, the intercept and slope of the leading Regge trajectory. In the forward direction then, (V. 3) receives significant contributions only from $|\underline{x}| \leq 0$ ($\log \eta_P$), and leads to an elastic cross section which saturates, but does not violate, the Froissart bound. In QED one finds that $M^{(1 \text{ chain})}(\underline{x}, \eta_P)$ possesses a fixed cut at $J = 1 + \frac{11\pi}{32} \alpha^2$ which is modulated by a complicated function of \underline{x} which behaves like $e^{-\lambda|\underline{x}|}$ for $|\underline{x}| \gg \frac{1}{\lambda}$. So, as in the case of $\lambda \phi^3$, although $M^{(1 \text{ chain})}$ taken alone violates the Froissart bound,

the Regge-eikonal formula leads to a cross section which increases only as $\log^2 \eta_P$. It is this phenomena which has led several authors to take the Regge-eikonal formula very seriously.

However, from the point of view of the physical picture developed in this paper it is not even clear that the Regge-eikonal scheme is at all reasonable. In particular, (V.2) assumes that the chains never interact among themselves. However, we have seen that the chains all scatter simultaneously off the external field, so they are really overlapping and crowded together in real space-time. So, even if the photons linking the pairs together were given a large mass (short range), such photons could easily propagate between two chains and link them up. The simplest example of such a process is shown in Fig. 12. This is an interference effect between a two-chain and a one-chain diagram. These will be studied in considerable detail in the next section.

VI. INTERFERENCE EFFECTS

We wish to consider the simplest type of interference graphs in some detail. These are the 2 chain-1 chain graphs, an example of which is drawn in Fig. 13. As in previous sections we are content to calculate only the leading logarithms of each diagram. In this approximation the photons forming the right hand chain in Fig. 13 are strongly ordered in the usual sense. This fact then allows us to formally sum over the subsections indicated by letters A, B, and C in Fig. 13 and replace them by their Regge form. This fact is stated pictorially in Fig. 14 where we have a Reggeon, defined diagrammatically in Fig. 15, interacting with an elementary particle (massive photon) through the exchange of another elementary particle. Just as in the calculation of the single chain, this exchange gives rise to an attractive potential between the particle and the Reggeon. Figure 14 has the

advantage of showing that this class of interference terms reduces to a quasi-two body calculation, and should, in principle, be solvable.

Although the single chain gives a fixed Regge cut in QED, there is no reason to restrict our considerations to just this case. We will, in fact, develop a formalism in which we can insert an input Reggeon (pole or cut) into Fig. 14, and then deduce some characteristics (energy dependence, at least) of the output Reggeon. In particular we will see cases in which Fig. 14 generates a scattering amplitude which grows faster with energy than the scattering amplitude corresponding to a single Regge exchange. Our method of analysis consists of several steps: first, write an integral equation which sums up diagrams of Fig. 14; second, specialize to the forward direction and obtain a simpler (Fredholm) integral equation; third, use variational principles to obtain lower bounds on the highest eigenvalue of the kernel; finally, relate the bound on the eigenvalue to a lower bound on the energy dependence of the scattering amplitude.

We begin the analysis by writing the S-matrix in a more convenient form. We define a function W which is related to the S-matrix by the removal of the photon legs 1, 2, 3, and 4 shown in Fig. 14. So,

$$\begin{aligned}
 S &= (2\pi)(2\eta) \delta(\eta - \eta') \int d\underline{p}_1 d\underline{\ell}_1 d\underline{q}_1 \delta(\underline{\Delta} - \underline{p}_1 - \underline{\ell}_1 - \underline{q}_1) \frac{d\alpha}{2\alpha} \int d\underline{p} d\underline{\ell} d\underline{q} \delta(\underline{\Delta} - \underline{p} - \underline{\ell} - \underline{q}) \\
 &\quad \left(\frac{1}{(\underline{\ell}_1^2 + \lambda^2)(\underline{q}_1^2 + \lambda^2)} \right) \left(\frac{1}{(\underline{\ell}^2 + \lambda^2)(\underline{q}^2 + \lambda^2)} \right) W \left(\underline{\ell}_1 + \underline{q}_1, \underline{p}_1; \underline{\ell} + \underline{q}, \underline{p}; \frac{\alpha}{\eta_{\min}} \right) \\
 S &= (2\pi)(2\eta) \delta(\eta - \eta') \int d\underline{p}_1 d\underline{\ell}_1 \frac{d\alpha}{2\alpha} \int d\underline{p} d\underline{\ell} \left(\frac{1}{[(\underline{\Delta} - \underline{p}_1 - \underline{\ell}_1)^2 + \lambda^2][\underline{\ell}_1^2 + \lambda^2]} \right) \\
 &\quad \left(\frac{1}{[(\underline{\Delta} - \underline{p} - \underline{\ell})^2 + \lambda^2][\underline{\ell}^2 + \lambda^2]} \right) W \left(\underline{\Delta} - \underline{p}_1, \underline{p}_1; \underline{\Delta} - \underline{p}, \underline{p}; \frac{\alpha}{\eta_{\min}} \right)
 \end{aligned}$$

The $\underline{\ell}$ and $\underline{\ell}_1$ integrals can be done, giving

$$S = (2\pi)(2\eta) \delta(\eta - \eta') \int d\underline{p}_1 \int d\underline{p} \int_{\eta_{\min}}^{\eta} \frac{d\alpha}{\alpha} k(|\underline{\Delta} - \underline{p}_1|) k(|\underline{\Delta} - \underline{p}|) W\left(\underline{\Delta} - \underline{p}_1, \underline{p}_1; \underline{\Delta} - \underline{p}, \underline{p}; \frac{\alpha}{\eta_{\min}}\right) \quad (\text{VI. 2})$$

where

$$k(|\underline{\Delta} - \underline{p}|) \equiv \int d\underline{\ell} \frac{1}{[(\underline{\Delta} - \underline{p}_1 - \underline{\ell}_1)^2 + \lambda^2][\underline{\ell}_1^2 + \lambda^2]} = \int d\underline{x} e^{-i(\underline{\Delta} - \underline{p}) \cdot \underline{x}} K_0^2(\mu|\underline{x}|) \quad (\text{VI. 3})$$

The function W now represents the propagation and interaction of the Reggeon and elementary particle in the t -channel. We can write an integral equation for W in terms of the Reggeon, the photon propagator and the interaction between them. The integral equation is represented pictorially in Fig. 16. If we represent the Reggeon by the function $R(\underline{k}, \eta/\eta_{\min})$, the integral equation becomes,

$$W\left(\underline{\Delta} - \underline{p}_1, \underline{p}_1; \underline{\Delta} - \underline{p}, \underline{p}; \frac{\eta}{\eta_{\min}}\right) = \delta(\underline{p} - \underline{p}_1) R\left(\underline{\Delta} - \underline{p}_1; \frac{\eta}{\eta_{\min}}\right) \frac{1}{(\underline{p}_1^2 + \lambda^2)} + \frac{e^4}{2(2\pi)^3} \int_{\eta_{\min}}^{\eta} \frac{d\alpha}{\alpha} \int \frac{d\underline{h}}{[(\underline{p}_1 - \underline{h})^2 + \lambda^2]} \frac{1}{(\underline{p}_1^2 + \lambda^2)} F(\underline{h} - \underline{p}_1, \underline{\Delta} - \underline{h}) R(\underline{\Delta} - \underline{p}_1, \eta/\alpha) F(\underline{p}_1, \underline{h} - \underline{p}_1) \times W\left(\underline{h}, \underline{\Delta} - \underline{h}; \underline{\Delta} - \underline{p}, \underline{p}; \frac{\alpha}{\eta_{\min}}\right) \quad (\text{VI. 4})$$

where the function F describes the possible momentum dependence in the coupling between the Reggeon and photon. By iterating (VI.4) one can verify that it indeed sums the diagrams of Fig. 13. Instead of discussing this integral equation in its

full generality we will specialize to a rather naive model in which F is momentum independent and R is a simple pole. The real situation in QED will be discussed at the end of this section.

With these simplifications the integral equation now reads,

$$\begin{aligned}
W(\underline{\Delta}-\underline{p}_1, \underline{p}_1; \underline{\Delta}-\underline{p}, \underline{p}; \frac{\eta}{\eta_{\min}}) &= \delta(\underline{p}-\underline{p}_1) \frac{1}{(\underline{p}_1^2 + \lambda^2)} \left(\frac{\eta}{\eta_{\min}}\right)^{\beta(\underline{\Delta}-\underline{p}_1)} \theta\left(\frac{\eta}{\eta_{\min}} - 1\right) \\
&+ \frac{e^4}{2(2\pi)^3} \int_{\eta_{\min}}^{\eta} \frac{d\alpha}{\alpha} \int \frac{d\underline{h}}{[(\underline{p}_1 - \underline{h})^2 + \lambda^2]} \frac{\lambda^2}{(\underline{p}_1^2 + \lambda^2)} \left(\frac{\eta}{\alpha}\right)^{\beta(\underline{\Delta}-\underline{p}_1)} W\left(\underline{h}, \underline{\Delta}-\underline{h}; \underline{\Delta}-\underline{p}, \underline{p}; \frac{\alpha}{\eta_{\min}}\right)
\end{aligned} \tag{VI.5}$$

where β is the trajectory function of the input Reggeon. W is, of course, different from zero only for $\eta/\eta_{\min} > 1$. It will suffice for the purposes at hand to consider the somewhat simpler integral equation for the function,

$$T(\underline{\Delta}-\underline{p}_1, \underline{p}_1; \frac{\eta}{\eta_{\min}}) = \int d\underline{p} k(|\underline{\Delta}-\underline{p}|) W(\underline{\Delta}-\underline{p}_1, \underline{p}_1; \underline{\Delta}-\underline{p}, \underline{p}; \frac{\alpha}{\eta_{\min}}) \tag{VI.6}$$

T satisfies the integral equation,

$$\begin{aligned}
T(\underline{\Delta}-\underline{p}_1, \underline{p}_1; \frac{\eta}{\eta_{\min}}) &= k(|\underline{\Delta}-\underline{p}_1|) \frac{1}{(\underline{p}_1^2 + \lambda^2)} \left(\frac{\eta}{\eta_{\min}}\right)^{\beta(\underline{\Delta}-\underline{p}_1)} \theta\left(\frac{\eta}{\eta_{\min}} - 1\right) \\
&+ \frac{e^4}{2(2\pi)^3} \int_{\eta_{\min}}^{\eta} \frac{d\alpha}{\alpha} \int \frac{d\underline{h}}{[(\underline{p}_1 - \underline{h})^2 + \lambda^2]} \frac{\lambda^2}{(\underline{p}_1^2 + \lambda^2)} \left(\frac{\eta}{\alpha}\right)^{\beta(\underline{\Delta}-\underline{p}_1)} T\left(\underline{h}, \underline{\Delta}-\underline{h}; \frac{\alpha}{\eta_{\min}}\right)
\end{aligned} \tag{VI.7}$$

Care must be taken in writing the order of the first two arguments in T, because this ordering reflects the exchange character of the interaction between the Reggeon and elementary particle. This integral equation becomes much simpler if we introduce Mellin transforms. Recall the definition of the transform,

$$T(\underline{\Delta}-\underline{p}, \underline{p}; J) = \int_0^{\infty} T(\underline{\Delta}-\underline{p}, \underline{p}; y) y^{-J-1} dy$$

and its inverse,

$$T(\underline{\Delta}-\underline{p}, \underline{p}; y) = \frac{1}{2\pi i} \int_C T(\underline{\Delta}-\underline{p}, \underline{p}; J) y^J dJ$$

where the contour is chosen to the right of all the singularities of $T(\underline{\Delta}-\underline{p}, \underline{p}; J)$.

It is an easy exercise to obtain the integral equation for the transforms,

$$T(\underline{\Delta}-\underline{p}_1, \underline{p}_1; J) = k(|\underline{\Delta}-\underline{p}_1|) \frac{1}{[J-\beta(\underline{\Delta}-\underline{p}_1)] [p_1^2 + \lambda^2]} + \frac{e^4}{2(2\pi)^3} \int \frac{d\tilde{h}}{[(\underline{p}_1 - \tilde{h})^2 + \lambda^2]} \frac{\lambda^2}{[p_1^2 + \lambda^2] [J-\beta(\underline{\Delta}-\underline{p}_1)]} T(\tilde{h}, \underline{\Delta}-\tilde{h}; J) \quad (\text{VI. 8})$$

Consider this equation in the forward ($\underline{\Delta}=0$) direction. The driving term then depends only upon p_1^2 . T will inherit this symmetry, so the angular integral in the homogeneous term can be done. If we carry out this integral and define,

$$t = p_1^2 \quad t' = \tilde{h}^2$$

the integral equation becomes,

$$T(t; J) = \frac{k(t)}{[J-\beta(t)] [t + \lambda^2]} + \frac{e^4}{4(2\pi)^2} \int_0^\infty \frac{dt'}{\sqrt{(t+t'+\lambda^2)^2 - 4tt'}} \frac{\lambda^2}{[t + \lambda^2] [J-\beta(t)]} T(t'; J) \quad (\text{VI. 9})$$

This one dimensional integral equation can be written with a symmetric kernel if we simply define,

$$W(t; J) = \sqrt{J-\beta(t)} \sqrt{t + \lambda^2} T(t; J) \quad (\text{VI. 10})$$

and note that

$$W(t; J) = \frac{k(t)}{\sqrt{J-\beta(t)} \sqrt{t + \lambda^2}} + \frac{e^4}{4(2\pi)^2} \int_0^\infty K_S(t, t') W(t'; J) d\left(\frac{t'}{\lambda^2}\right) \quad (\text{VI. 11})$$

where

$$K_S(t, t') = \left(\frac{1}{\sqrt{J-\beta(t)} \sqrt{t+\lambda^2}} \right) \left(\frac{\lambda^4}{\sqrt{(t+t'+\lambda^2)^2 - 4tt'}} \right) \left(\frac{1}{\sqrt{J-\beta(t')} \sqrt{t'+\lambda^2}} \right) \quad (\text{VI. 12})$$

Since $K_S(t, t')$ is a symmetric, real, square-integrable kernel, it must have a discrete spectrum of real eigenvalues.⁸ It will become evident shortly that if we can obtain the highest eigenvalue of K_S , then we will have found the leading energy dependence of the set of graphs of interest. Actually, we will be content to obtain a rather weak lower bound on the highest eigenvalue of K_S and thereby obtain a lower bound on the energy dependence of the amplitude.

In order to see explicitly the connection between the eigenvalue problem and the energy dependence of the scattering amplitude we go back to (VI.2) and write it in terms of $W(t; J)$. From (VI.2) and (VI.3) we have

$$S = (2\pi)(2\eta) \delta(\eta - \eta') \int_{\eta_{\min}}^{\eta} dp_1 \frac{d\alpha}{\alpha} k(|\Delta - p_1|) T(\Delta - p_1, p_1; \frac{\alpha}{\eta_{\min}}) \quad (\text{VI. 13})$$

Then, introducing Mellin transforms and specializing to the forward direction, we have using (VI.10)

$$S = (2\pi)(2\eta) \delta(\eta - \eta') M\left(\frac{\eta}{\eta_{\min}}\right) \quad (\text{VI. 14})$$

where, for large η/η_{\min} ,

$$M\left(\frac{\eta}{\eta_{\min}}\right) = \pi \int_0^{\infty} dt k(t) \int_C \frac{W(t; J)}{J\sqrt{J-\beta(t)}\sqrt{t+\lambda^2}} \left(\frac{\eta}{\eta_{\min}}\right)^J dJ \quad (\text{VI. 15})$$

where the contour C lies to the right of all the singularities of the integrand.

Consider the integral equation for W and write it schematically,

$$W = B + g K_S W \quad (\text{VI. 16})$$

where $g = \frac{e^4}{4(2\pi)^2}$. (VI.16) has the formal solution

$$W = (1 - g K_S)^{-1} B \quad (\text{VI.17})$$

which may be written under appropriate circumstances⁸ as a series,

$$W(t; J) = \sum_{n=0}^{\infty} W^{(n)}(t; J) = \sum_{n=0}^{\infty} (g K_S)^{(n)} B \quad (\text{VI.18})$$

The n th approximate of $W(t; J)$ is given by

$$W^{(n)}(t; J) = g^n \int \dots \int dt_1 \dots dt_n K_S(t, t_1) K_S(t_1, t_2) \dots K_S(t_{n-1}, t_n) B(t_n) \quad (\text{VI.19})$$

Since K_S is a Fredholm kernel it has a discrete spectral decomposition,⁸

$$K_S(t, t') = \sum_{n=1}^{\infty} \mu_n f_n(t) f_n(t') \quad (\text{VI.20})$$

where μ_n and $f_n(t)$ are respectively the n th eigenvalue and eigenfunction of K_S .

If we then approximate $W^{(n)}(t; J)$ by withholding only the highest eigenvalue (μ_1) of K_S , (VI.19) becomes,

$$W^{(n)}(t; J) \sim g^n \mu_1^n(J) f_1(t; J) \int dt' f_1(t'; J) B(t') \quad (\text{VI.21})$$

where we have indicated explicitly that the eigenvalues and eigenfunctions can depend upon J . If we now introduce the Mellin transform of $M\left(\frac{\eta}{\eta_{\min}}\right)$,

$$M(J) = \pi \int_0^{\infty} dt k(t) \frac{W(t; J)}{J \sqrt{J - \beta(t)} \sqrt{t + \lambda}^2} \quad (\text{VI.22})$$

we have from (VI.21) that its n th approximate is,

$$M^{(n)}(J) \sim g^n \mu_1^n(J) \left[\int_0^{\infty} dt \frac{f_1(t; J)}{J \sqrt{J - \beta(t)} \sqrt{t + \lambda}^2} \right] \left[\int_0^{\infty} dt' f_1(t'; J) B(t') \right] \quad (\text{VI.23})$$

Therefore, summing over n,

$$M(J) = \sum_{n=0}^{\infty} M^{(n)}(J) = \left(\frac{1}{1-g\mu_1(J)} \right) \left[\int_0^{\infty} dt \frac{f_1(t;J)}{J\sqrt{J-\beta(t)}\sqrt{t+\lambda^2}} \right] \left[\int_0^{\infty} dt' f_1(t';J)B(t') \right] \quad (\text{VI.24})$$

So, it is clear that M(J) will develop a pole at $J=J_0$ where

$$1 - g\mu_1(J_0) = 0 \quad (\text{VI.25})$$

By doing a simple variational calculation to obtain a lower bound on $\mu_1(J_0)$, we can obtain estimates of the location of the solution J_0 of (VI.25).

Recall the Rayleigh-Reitz variational principle which states that the largest eigenvalue of K_S is given by

$$\mu_1 = \sup_{f \in L_2} \frac{(f(t), K_S(t, t')f(t'))}{(f(t), f(t))} \quad (\text{VI.26})$$

where $f(t)$ is any square integrable function. So, if we choose $f(t)$ at random, we can be sure that (VI.26) will give a lower bound on μ_1 . We choose,

$$f(t) = \frac{1}{\lambda} \sqrt{J-\beta(t)} \sqrt{t+\lambda^2} e^{-at} \quad (\text{VI.27})$$

where "a" is a parameter which must be chosen such that $f(t)$ is normalized to unity. From (VI.12) and (VI.27), we compute

$$(f, K_S f) = \frac{1}{\lambda^2} \int dt dt' \frac{e^{-a(t+t')}}{\sqrt{(t+t'+\lambda^2)^2 - 4tt'}} \quad (\text{VI.28})$$

By changing the integration variables to $t_+ = t+t'$ and $t_- = t-t'$, it is not difficult to reduce (VI.28) to a one dimensional integral,

$$(f, K_S f) = \frac{1}{2a\lambda^2} e^{-\frac{1}{2}a\lambda^2} \int_{(a\lambda^2/2)}^{\infty} e^{-y} y^{-1} dy \quad (\text{VI.29})$$

The relation between "a" and J is given in this approach by the normalization condition,

$$(f, f) = 1 = \frac{1}{\lambda^4} \int_0^{\infty} [J - \beta(t)] [t + \lambda^2] e^{-2at} dt \quad (\text{VI. 30})$$

We suppose for illustration that the trajectory is linear, $\beta(t) = \beta_0 - \beta_1 t$. Then,

$$(f, f) = (J - \beta_0) \frac{1}{(2a\lambda^2)} + (J - \beta_0 + \beta_1 \lambda^2) \frac{2}{(2a\lambda^2)^2} + \beta_1 \lambda^2 \frac{6}{(2a\lambda^2)^3} \quad (\text{VI. 31})$$

Two extreme cases of (VI. 29) and (VI. 31) are quite simple and illustrate clearly the mechanism at work. First consider $(a\lambda^2) \gg 1$. Then

$$(f, K_S f) \sim \frac{1}{(a\lambda^2)^2} \quad (f, f) \sim \frac{J - \beta_0}{2(a\lambda^2)} = 1 \quad (\text{VI. 32})$$

Thus,

$$\mu_1(J) > \sqrt{\frac{2}{J - \beta_0}} \quad (\text{VI. 33})$$

Inserting this inequality into (VI. 25), we find that $M(J)$ develops a pole at

$$J_0 > \beta_0 + 2g^2 \quad (\text{VI. 34})$$

which is further to the right on the complex J-plane than the input Reggeon pole which is located at $J = \beta_0$. We cannot take this example too seriously, however, because it corresponds to strong coupling. However, we can consider another case which is closer to QED. Imagine that $(a\lambda^2)$ is small and $\beta_1 = 0$. Then,

$$(f, K_S f) = \frac{1}{2a\lambda^2} \log\left(\frac{2}{a\lambda^2}\right) > \frac{1}{2a\lambda^2}, \quad (f, f) = \frac{2(J - \beta_0)}{(2a\lambda^2)^2} \quad (\text{VI. 35})$$

So,

$$\mu_1(J) > \frac{1}{\sqrt{2(J - \beta_0)}}$$

which means, according to (VI. 25), that

$$J_0 > \beta_0 + \frac{g^2}{2} \quad (\text{VI. 36})$$

in this weak coupling case.

These two very crude examples serve to illustrate the point that it is not difficult to find t channel exchanges which lead to stronger energy dependences than simple chains. The relation, however, of these model calculations to QED is more delicate. As we saw in Section III, the chain diagrams in QED generate a Regge cut, which we have written as a linear superposition of poles. In principle, we can treat this case because our integral equation is also linear. Another difference between QED and the model calculation is that the coupling between the Regge cut and the photon is actually momentum dependent. This fact could change the character of the integral equation, but it does not change the fact that the exchanged photons in Fig. 14 tend to bind the t -channel system. So, although the spectrum of $K_S(t, t')$ may no longer be discrete, diagrams like Fig. 14 could still possess a stronger energy dependence than the simple chain.

Potentially more interesting than the 2 chain-1 chain diagrams considered here are the 2 chain-2 chain diagrams. We can give these a pictorial representation shown in Fig. 17, and recognize that they are iterated Mandelstam cut diagrams. Such diagrams have been considered in the literature and it has been conjectured that they generate Regge poles, although this point has not been verified.⁹

VII. CONCLUSIONS AND DISCUSSION

Guided by a clear physical picture, we have accumulated evidence that graphs more complicated than simple multiperipheral chains might play a substantial role in diffraction scattering. One might now take the diagrams of Fig. 14 and use them as the input of the s -channel iteration procedure described in Section V. Since these diagrams have a stronger energy dependence than the single multiperipheral chains, they certainly give a significant contribution to

the S-matrix. We cannot, however, claim that they contribute significantly to the total cross section since this quantity depends upon the range of the graphs in the transverse $|\underline{x}|$ plane (which we have not determined) as well as their energy dependence. More importantly, however, we have argued that the s-channel iteration scheme is not a physically convincing procedure. So, we do not take this proposal seriously. It appears that present field theoretic approaches to diffraction scattering lack a compelling mechanism to enforce s-channel unitarity. Until this deep problem is understood more clearly, detailed perturbation theory calculations will not resolve additional really interesting and important questions in this field.

The results of this paper suffer from the technical limitation in any leading logarithm calculation. It has been argued¹⁰ that leading logarithm calculations are only accurate when the couplings of the particles are small enough. However, the spirit of this investigation is to obtain results which do not rely upon the size of coupling constants. It is the unspoken hope of this investigation that although the leading logarithm approach is not perfectly accurate, it remains indicative of the truth if the coupling constants become fairly large. One might argue, for example, that it would certainly be bizarre if the energy dependence of the interference terms decreased relative to the single multiperipheral chain as the coupling constant increased! One might also question the usefulness of perturbation theory in this entire program. We saw in Section III that the single multiperipheral chain violates the Froissart bound by a power of the energy. The s-channel iteration procedure then reduced the energy dependence of the scattering amplitude until it just saturated the bound. However, the success of this procedure relied upon the detailed cancellation among graphs, each of which was absurdly large. One might now ask whether this feat was profound or accidental. For example, are there other graphs which further reduce the energy dependence

of the final result?

We have emphasized our space-time picture of high energy scattering throughout this paper. In particular we have argued in Section V that it is not unlikely for two particles in the physical state of the projectile to possess small relative subenergy and to propagate near one another. These conditions are, however, the ideal ones in which the particles are likely to interact significantly (e.g., resonant). This is a problem which exists (and is often ignored) even in multiperipheral models in which only one chain of constituents is allowed. However, this effect can reach extreme proportions for physical particle states consisting of more than one chain of constituents. For example, e^+e^- pairs on different chains are likely to overlap in both momentum and configuration space. These pairs will certainly interact and their respective chains might often be linked up in the process. A simple example of such a possibility is shown in Fig. 18. Unfortunately, perturbation theory is not an efficient tool for computing these effects. Perhaps the effective field technique from statistical physics provides a better calculational and conceptual framework for this problem. Anyway, in light of the complexity of Section VI, more theoretical effort is needed in deciding questions of this general nature than in the calculations of minute details of diagrams which just happen to be exactly computable.

Acknowledgement

The author would like to thank J. D. Bjorken for many helpful discussions and guidance during the course of this research. Conversations with D. E. Soper and the theory group at SLAC are also acknowledged.

APPENDIX A. SINGLE LOOP

In this Appendix we will illustrate our calculational methods by extracting the leading energy dependence of the simplest graph in the class to be considered. According to our perturbation theory there are four diagrams (Fig.2). However, if we recall that the infinite momentum polarization vectors satisfy

$$-g^{\mu\nu} = \sum_{\lambda=1}^2 \epsilon_{\lambda}^{\mu}(p) \epsilon_{\lambda}^{\nu}(p) + \frac{1}{\eta^2} (2\eta_{H-\underline{p}}^2) \delta_3^{\mu} \delta_3^{\nu} \quad (\text{A. 1})$$

it is easy to see that the four diagrams can be combined into one (Fig.3). Now, however, instead of associating a factor $\sum_{\lambda} \epsilon_{\lambda}^{\mu}(p) \epsilon_{\lambda}^{\nu}(p)$ with each internal photon we make the association with $-g^{\mu\nu}$. Throughout this paper this simplification of our perturbation theory rules will be tacitly understood.

Now it is straightforward to write down the amplitude for this diagram. Since this diagram has been studied previously in the literature by Cheng and Wu⁴, and others⁵, we will try to use notation as similar to theirs as possible. Using the kinematics indicated in Fig.5.,

$$\begin{aligned} S^{(1)} = & \frac{e^4}{(2\pi)^9} \delta(\eta_{\underline{P}} - \eta_{\underline{P}'}) \int d\underline{p} d\underline{k}_1 d\underline{p}_1 d\underline{p}_4 d\underline{\eta}_{k_1} d\underline{\eta}_1 (2\eta)^{-2} (2\eta_{k_1})^{-2} (2\eta_1)^{-2} (2\eta_2)^{-2} \\ & [H(\underline{P}) - H(\underline{p}) - \omega(k_1)]^{-1} [H(\underline{P}) - H(\underline{p}) - H(\underline{p}_1) - H(\underline{p}_2)]^{-1} [H(\underline{P}') - H(\underline{p}') - \omega(k_2)]^{-1} \\ & [H(\underline{P}') - H(\underline{p}') - H(\underline{p}_3) - H(\underline{p}_4)]^{-1} \sum_{\underline{s}, \underline{s}'} \bar{u}(\underline{P}'\underline{s}') \gamma^{\sigma}_{u(\underline{p}', \underline{s}')} \bar{u}(\underline{p}', \underline{s}') \gamma^0_{u(\underline{p}, \underline{s})} \\ & \bar{u}(\underline{p}, \underline{s}) \gamma^{\mu}_{u(\underline{P}, \underline{s})} \text{tr} [(\not{p}'_1 + m) \gamma^0 (\not{p}'_4 + m) \gamma_{\sigma} (-\not{p}'_3 + m) \gamma^0 (-\not{p}'_2 + m) \gamma_{\mu}] \\ & [F(\underline{p}' - \underline{p}) F(\underline{p}_4 - \underline{p}_1) F_c(\underline{p}_3 - \underline{p}_2) - (2\pi)^6 \delta(\underline{p}' - \underline{p}) \delta(\underline{p}_4 - \underline{p}_1) \delta(\underline{p}_3 - \underline{p}_2)] \end{aligned} \quad (\text{A. 2})$$

where

$$\begin{aligned}
(\underline{p}, \eta) &= (\underline{P}-\underline{k}, \eta_{\underline{P}}-\eta_{\underline{k}_1}) & , & & (\underline{k}_2, \eta_{\underline{k}_2}) &= (\underline{P}'-\underline{p}', \eta_{\underline{P}'}-\eta') \\
(\underline{p}_2, \eta_2) &= (\underline{k}_1-\underline{p}_1, \eta_{\underline{k}_1}-\eta_1) & , & & (\underline{p}_3, \eta_3) &= (\underline{P}'-\underline{p}'-\underline{p}_4, \eta_{\underline{P}'}-\eta'-\eta_4)
\end{aligned}$$

Since we are involved in a leading log calculation, we should treat the external field perturbatively. Through fourth order the possible diagrams are listed in Fig.4a and b. However, the diagrams in Fig.4a prove to be larger than those in Fig.4b by a factor of $\log \eta_{\underline{p}}$, so we will limit our attention to them. Now expanding the eikonal factor in (A. 2) and withholding only the appropriate terms,

$$\begin{aligned}
& [F(\underline{p}'-\underline{p}) F(\underline{p}_4-\underline{p}_1) F_c(\underline{p}_3-\underline{p}_2) (2\pi)^6 \delta(\underline{p}'-\underline{p}) \delta(\underline{p}_4-\underline{p}_1) \delta(\underline{p}_3-\underline{p}_2)] = \\
& (2\pi)^2 \delta(\underline{p}'-\underline{p}) e^4 \left\{ \frac{1}{[(\underline{p}_4-\underline{p}_1)^2 + \lambda^2][(\underline{p}_3-\underline{p}_2)^2 + \lambda^2]} - \frac{1}{2} \delta(\underline{p}_4-\underline{p}_1) \int d\underline{q} \frac{1}{[\underline{q}^2 + \lambda^2][(\underline{p}_3-\underline{p}_2-\underline{q})^2 + \lambda^2]} \right. \\
& \left. - \frac{1}{2} \delta(\underline{p}_3-\underline{p}_2) \int d\underline{q} \frac{1}{[\underline{q}^2 + \lambda^2][(\underline{p}_4-\underline{p}_1-\underline{q})^2 + \lambda^2]} \right\} \quad (A. 3)
\end{aligned}$$

Substituting this into (A. 2) we have,

$$\begin{aligned}
S^{(1)} &= \frac{e^8}{(2\pi)^7} \delta(\eta_{\underline{P}}-\eta_{\underline{P}'}) \int d\underline{k}_1 d\underline{p}_1 d\underline{p}_4 d\underline{\eta}_{\underline{k}_1} d\underline{\eta}_1 (2\eta)^{-2} (2\eta_{\underline{k}_1})^{-2} (2\eta_1)^{-2} (2\eta_2)^{-2} \\
& [H(\underline{P})-H(\underline{p})-\omega(\underline{k}_1)]^{-1} [H(\underline{P})-H(\underline{p})-H(\underline{p}_1)-H(\underline{p}_2)]^{-1} [H(\underline{P}')-H(\underline{p}')-\omega(\underline{k}_2)]^{-1} \\
& [H(\underline{P}')-H(\underline{p}')-H(\underline{p}_3)-H(\underline{p}_4)]^{-1} \sum_{\underline{s}, \underline{s}'} \bar{u}(\underline{P}'\underline{s}') \gamma^\sigma u(\underline{p}', \underline{s}') \bar{u}(\underline{p}'\underline{s}') \gamma^0 u(\underline{p}, \underline{s}) \bar{u}(\underline{p}, \underline{s}) \gamma^\mu u(\underline{P}, \underline{S}) \\
& \text{tr} [(\not{\underline{p}}_1 + \underline{m}) \gamma^0 (\not{\underline{p}}_4 + \underline{m}) \gamma_\sigma (-\not{\underline{p}}_3 + \underline{m}) \gamma^0 (-\not{\underline{p}}_2 + \underline{m}) \gamma_\mu] \left\{ \frac{2}{[(\underline{p}_4-\underline{p}_1)^2 + \lambda^2][(\underline{p}_3-\underline{p}_2)^2 + \lambda^2]} - \right.
\end{aligned}$$

$$\left. \begin{aligned} & \delta(p_4 - p_1) \int dq \frac{1}{[q^2 + \lambda^2] [(p_3 - p_2 - q)^2 + \lambda^2]} - \delta(p_4 - p_1) \int dq \frac{1}{[q^2 + \lambda^2] [(p_4 - p_1 - q)^2 + \lambda^2]} \end{aligned} \right\} \quad (\text{A. 4})$$

It is not difficult to infer from (A. 4) that the region $\eta_{k_1} \ll \eta_P$ of phase space gives the dominant contribution to the scattering amplitude. Furthermore, in this region of phase space the sum over the indices σ and μ receive their dominant contributions from the values $\sigma = \mu = 0$ (upper indices!). This fact can be checked in detail, and can be understood from the observation that γ^0 scales like η under z boosts (favoring large η in the through-going electron line), and γ^3 scales like H under z boosts (favoring small η for the virtual photons). And lastly we can neglect $H(P)$ and $H(p')$ in all the energy denominators since they are $O(\frac{1}{\eta_P})$. These observations lead to simplifications of many factors in S_{fi} :

$$\bar{u}(p, s) \gamma^0 u(P, S) = 2\sqrt{\eta_P \eta} \quad \delta_{Ss} \approx 2\eta_P \delta_{Ss}$$

$$H(P) - H(p) - \omega(k_1) \approx -\omega(k_1) = -\frac{k_1^2 + \lambda^2}{2\eta_{k_1}} \quad (\text{A. 5})$$

$$H(P) - H(p) - H(p_1) - H(p_2) \approx -H(p_1) - H(p_2) = -\frac{p_1^2 + m^2}{2\eta_1} - \frac{p_2^2 + m^2}{2\eta_2}$$

It will prove convenient to scale the η dependence out of the integrand, so introduce the dimensionless variables α and β ,

$$\eta_{k_1} = \alpha \eta_P \quad , \quad \eta_1 = \beta \eta_{k_1} = \beta(\alpha \eta_P)$$

where

$$0 \leq \alpha \leq 1 \quad , \quad 0 \leq \beta \leq 1$$

Now,

$$\begin{aligned}
S^{(1)} \cong & \frac{e^{\delta}}{2(2\pi)^7} \eta_P \delta(\eta_P - \eta_{P'}) \delta_{SS'} \int d\tilde{k}_1 d\tilde{p}_1 d\tilde{p}_4 \frac{d\alpha}{\alpha} d\beta [k_1^2 + \lambda^2]^{-1} [k_2^2 + \lambda^2]^{-1} \\
& \frac{\text{tr} [(\not{p}_1 + m) \gamma^0 (\not{p}_4 + m) \gamma^3 (-\not{p}_3 + m) \gamma^0 (-\not{p}_2 + m) \gamma^3]}{[(1-\beta)(p_1^2 + m^2) + \beta(p_2^2 + m^2)] [(1-\beta)(p_4^2 + m^2) + \beta(p_3^2 + m^2)]} \\
& \left\{ \frac{1}{[(p_4 - p_1)^2 + \lambda^2] [(p_3 - p_2)^2 + \lambda^2]} - \frac{1}{2} \delta(p_4 - p_1) \int d\tilde{q} \frac{1}{[q^2 + \lambda^2] [(p_3 - p_2 - q)^2 + \lambda^2]} - \right. \\
& \left. \frac{1}{2} \delta(p_3 - p_2) \int d\tilde{q} \frac{1}{[q^2 + \lambda^2] [(p_4 - p_1 - q)^2 + \lambda^2]} \right\} \quad (\text{A.6})
\end{aligned}$$

This expression becomes considerably more transparent if we change integration variables. First choose a frame such that

$$\tilde{P}' = -\tilde{P}$$

and define new integration variables \tilde{q} and \tilde{q}' ,

$$\tilde{k}_1 = \tilde{P} + \tilde{q} \quad , \quad \tilde{p}_4 = \tilde{P}' + \tilde{p}_1 - \tilde{q}'$$

Furthermore, if we introduce a function

$$\begin{aligned}
K(\tilde{P}'; \tilde{q}, \tilde{q}') = & \frac{e^4}{2(2\pi)^4} \int d\tilde{p}_1 d\beta \left\{ \frac{\text{tr} [(\not{p}_1 + m) \gamma^0 (\not{P}' - \not{q}' + \not{p}_1 + m) \gamma^3 (\not{p}_1 + \not{q} - \not{q}' + m) \gamma^0 (\not{p}_1 + \not{P}' - \not{q} + m) \gamma^3]}{[(1-\beta)p_1^2 + \beta(P' - q + p_1)^2 + m^2] [(1-\beta)(P' - q' + p_1)^2 + \beta(q' - q - p_1)^2 + m^2]} \right. \\
& \left. + (q' = P') + (q' = -P') \right\} \quad (\text{A.7})
\end{aligned}$$

the scattering amplitude can be written in the form,

$$S^{(1)} = (2\pi e^4)^2 \eta_P \delta(\eta_P - \eta_{P'}) \delta_{SS'} \int \frac{d\mathbf{q}}{(2\pi)^2} \frac{d\mathbf{q}'}{(2\pi)^2} \frac{d\alpha}{\alpha} \left[(\mathbf{P}' - \mathbf{q})^2 + \lambda^2 \right]^{-1} \left[(\mathbf{P}' + \mathbf{q})^2 + \lambda^2 \right]^{-1} \\ \left[(\mathbf{P}' - \mathbf{q}')^2 + \lambda^2 \right]^{-1} \left[(\mathbf{P}' + \mathbf{q}')^2 + \lambda^2 \right]^{-1} K(\mathbf{P}'; \mathbf{q}, \mathbf{q}') \quad (\text{A. 8})$$

We see from this expression that the function K describes the composition of the virtual photon as a bare pair, and predicts how effectively such a system scatters off an external field. This function has been obtained and simplified previously by Frolov et. al.⁵, and Cheng and Wu.⁴ Our analysis agrees with theirs, and after a lengthy Feynman parameter calculation we find,

$$K(0; \mathbf{q}, \mathbf{q}') = \left(\frac{8\alpha^2}{\pi} \right) \int_0^1 dx \int_0^1 dy \frac{[x(1-x) + y(1-y)] q^2 q'^2 - 2x(1-x)y(1-y) [2q^2 q'^2 + (\mathbf{q} \cdot \mathbf{q}')^2]}{x(1-x)q^2 + y(1-y)q'^2 + m^2} \quad (\text{A. 9})$$

in the forward direction.

We want only to observe at this time that K does not depend upon α . Hence, the scattering amplitude apparently diverges logarithmically. However, an improved analysis of this process (our method, for instance, interchanges limits and integrations freely) shows that the α integral should be cutoff at the point where the virtual photon is becoming "wee." Such a procedure is physically sensible since the pair intermediate state is no longer long-lived once the photon's longitudinal momentum falls to order unity. Thus,

$$\int \frac{d\alpha}{\alpha} \rightarrow \int_{\frac{\eta_{\min}}{\eta_P}}^1 \frac{d\alpha}{\alpha} = \log \left(\frac{\eta_P}{\eta_{\min}} \right) \quad (\text{A. 10})$$

The scattering amplitude depends logarithmically on the energy of the incident electron,

$$S^{(1)} = - (8\pi e^4) \eta_P \log \eta_P \delta(\eta_P - \eta_{P'}) \delta_{SS'} \int \frac{dq}{(2\pi)^2} \frac{dq'}{(2\pi)^2} \left[(\underline{P}' - \underline{q})^2 + \lambda^2 \right]^{-1} \left[(\underline{P}' + \underline{q})^2 + \lambda^2 \right]^{-1} \\ \left[(\underline{P}' - \underline{q}')^2 + \lambda^2 \right]^{-1} \left[(\underline{P}' + \underline{q}')^2 + \lambda^2 \right]^{-1} K(\underline{P}'; \underline{q}, \underline{q}') \quad (\text{A. 11})$$

For later analysis it will prove useful to define

$$M^{(1)} = -e^4 \log \eta_P \delta_{S'S} \int \frac{dq}{(2\pi)^2} \frac{dq'}{(2\pi)^2} \left[(\underline{P}' - \underline{q})^2 + \lambda^2 \right]^{-1} \left[(\underline{P}' + \underline{q})^2 + \lambda^2 \right]^{-1} \left[(\underline{P}' - \underline{q}')^2 + \lambda^2 \right]^{-1} \\ \left[(\underline{P}' + \underline{q}')^2 + \lambda^2 \right]^{-1} K(\underline{P}'; \underline{q}, \underline{q}') \quad (\text{A. 12})$$

and write,

$$S^{(1)} = 2\eta_P (2\pi) \delta(\eta_P - \eta_{P'}) M^{(1)} \quad (\text{A. 13})$$

APPENDIX B. SINGLE CHAIN

We wish to study the multiperipheral diagrams in Fig.6 and indicate the arguments necessary to obtain the amplitude for a chain of $N e^+ e^-$ pairs in Fig.7. In placing the eikonal vertices on just the second pair in Fig.6 we have anticipated the fact that the external field will be treated perturbatively as in the previous section, and only the leading behavior of the diagram will be found. According to our perturbation theory rules the amplitude for Fig.6a reads,

$$\begin{aligned}
 S_a^{(2)} &= -\frac{e^8}{(2\pi)^{13}} \delta(\eta_P - \eta_{P'}) \int dk_1 dp_1 d\eta_{k_1} d\eta_1 (2\eta_{k_1})^{-2} (2\eta_1)^{-2} (2\eta_2)^{-2} (2\eta)^{-2} \\
 & \left[H(P) - H(p) - \omega(k_1) \right]^{-1} \left[H(P) - H(p) - H(p_1) - H(p_2) \right]^{-1} \left[H(P') - H(p) - \omega(k_2) \right]^{-1} \left[H(P') - H(p) - H(p_3) - H(p_4) \right]^{-1} \\
 & \sum_{s, s'} \bar{u}(P', S') \gamma^\nu u(p, s) \bar{u}(p, s) \gamma^\mu u(P, S) \text{tr}[(\not{p}_1 + m) \gamma^\rho (\not{p}_4 + m) \gamma_\nu (-\not{p}_3 + m) \gamma^\sigma (-\not{p}_2 + m) \gamma_\mu] \\
 & dk_3 dp_5 dp_8 d\eta_{k_3} d\eta_5 (2\eta_{k_3})^{-2} (2\eta_5)^{-2} (2\eta_6)^{-2} \left[H(P) - H(p) - H(p_2) - H(p_4) - \omega(k_3) \right]^{-1} \\
 & \left[H(P) - H(p) - H(p_4) - H(p_2) - H(p_5) - H(p_6) \right]^{-1} \left[H(P') - H(p) - H(p_2) - H(p_4) - \omega(k_4) \right]^{-1} \\
 & \left[H(P') - H(p) - H(p_4) - H(p_2) - H(p_8) - H(p_7) \right]^{-1} \text{tr}[(\not{p}_5 + m) \gamma^0 (\not{p}_8 + m) \gamma_\sigma (-\not{p}_7 + m) \gamma^0 (-\not{p}_6 + m) \gamma_\rho] \\
 & \left[F(\not{p}_8 - \not{p}_5) F_c(\not{p}_7 - \not{p}_6) - (2\pi)^2 \delta(\not{p}_8 - \not{p}_5) \delta(\not{p}_7 - \not{p}_6) \right] \tag{B.1}
 \end{aligned}$$

The overall minus sign occurs because photon 3 attaches to an electron line while photon 4 attaches to a positron. Clearly $S^{(2)}$ is in general untractable.

However, as we expect on the basis of the analysis of the previous Appendix,

$S^{(2)}$ receives its dominant η dependence from that region of phase space where

$$\eta_{k_1} \ll \eta_P \quad , \quad \eta_{k_3} \ll \eta_2$$

This means, in the language of multiperipheral models, that only strongly-ordered diagrams contribute to the calculation. Furthermore, in this region of phase space we can set

$$\mu = \nu = \rho = \sigma = 0 \quad (\text{upper indices!})$$

and approximate the energy denominators,

$$H(P) - H(p) - \omega(k_1) \approx -\omega(k_1)$$

$$H(P) - H(p) - H(p_4) - H(p_2) - H(p_5) - H(p_6) \approx -H(p_5) - H(p_6) \quad , \text{etc.}$$

The amplitude simplifies to read,

$$S^{(2)} = - \frac{e^8}{(2\pi)^{13}} (\eta_P - \eta_P) \int dk_1 dp_1 d\eta_{k_1} d\eta_1 (2\eta_{k_1})^{-2} (2\eta_1)^{-2} (2\eta_2)^{-2} (2\eta)^{-2}$$

$$\left[\omega(k_1) \right]^{-1} \left[\omega(k_2) \right]^{-1} \left[H(p_1) + H(p_2) \right]^{-1} \left[H(p_3) + H(p_4) \right]^{-1}$$

$$\sum_{s, s'} \bar{u}(P', S') \gamma^0_u(p, s) \bar{u}(p, s) \gamma^0_u(P, S) \text{tr} \left[(\not{p}_1 + m) \gamma^0 (\not{p}_4 + m) \gamma^3 (-\not{p}_3 + m) \gamma^0 (-\not{p}_2 + m) \gamma^3 \right]$$

$$dk_3 dp_5 dp_8 d\eta_{k_3} d\eta_5 (2\eta_{k_3})^{-2} (2\eta_5)^{-2} (2\eta_6)^{-2} \left[\omega(k_3) \right]^{-1} \left[\omega(k_4) \right]^{-1} \left[H(p_5) + H(p_6) \right]^{-1}$$

$$\left[H(p_7) + H(p_8) \right]^{-1} \text{tr} \left[(\not{p}_5 + m) \gamma^0 (\not{p}_8 + m) \gamma^3 (-\not{p}_7 + m) \gamma^0 (-\not{p}_6 + m) \gamma^3 \right]$$

$$\left[F_{\not{p}_8 - \not{p}_5} F_c(\not{p}_7 - \not{p}_6) - (2\pi)^2 \delta(\not{p}_8 - \not{p}_5) \delta(\not{p}_7 - \not{p}_6) \right] \quad (\text{B. 2})$$

Treating the eikonal perturbatively and introducing integration variables for the "lower" loop as we did for Fig.5,

$$\begin{aligned} \underline{k}_3 &= \underline{P} + \underline{q}' & \underline{p}_8 &= \underline{P}' + \underline{p}_5 - \underline{q}'' \\ \eta_{k_3} &= \gamma \eta_P & \eta_5 &= \delta \eta_{k_3} = \delta(\gamma \eta_P) \end{aligned}$$

we can identify a factor of $-K$ coming from the lower loop

$$\begin{aligned} S^{(2)} &= \frac{e^8}{(2\pi)^5} 2\delta(\eta_P - \eta_{P'}) \int d\underline{k}_1 d\underline{p}_1 d\underline{\eta}_{k_1} d\underline{\eta}_1 \theta(\eta - \eta_{k_1}) \theta(\eta_1 - \eta_{k_3}) (2\eta_{k_1})^{-2} (2\eta_1)^{-2} (2\eta_2)^{-2} \\ & (2\eta)^{-1} [\omega(k_1)]^{-1} [\omega(k_2)]^{-1} [H(p_1) + H(p_2)]^{-1} [H(p_3) + H(p_4)]^{-1} \sum_{s, s'} \bar{u}(P', S') \gamma_u^0(p, s) \bar{u}(p, s) \gamma_u^0(P, S) \\ & \text{tr}[(\not{p}_1 + m) \gamma^0 (\not{p}_4 + m) \gamma^3 (-\not{p}_3 + m) \gamma^0 (-\not{p}_2 + m) \gamma^3] \frac{d\gamma}{\gamma} d\underline{q}' d\underline{q}'' [(\underline{P}' - \underline{q}')^2 + \lambda^2]^{-1} \\ & [(\underline{P}' + \underline{q})^2 + \lambda^2]^{-1} [(\underline{P}' - \underline{q}'')^2 + \lambda^2]^{-1} [(\underline{P}' + \underline{q}'')^2 + \lambda^2]^{-1} K(\underline{P}'; \underline{q}', \underline{q}'') \end{aligned} \quad (\text{B. 3})$$

where the θ functions enforce the fact that all the η 's in the diagram must be positive. If we now change variables in the "upper" loop in the usual way,

$$\begin{aligned} \underline{k}_1 &= \underline{P} + \underline{q} & \underline{p}_1 &= \underline{P}' + \underline{p}_4 - \underline{q}' \\ \eta_{k_1} &= \alpha \eta_P & \eta_1 &= \beta \eta_{k_1} = \beta(\alpha \eta_P) \end{aligned}$$

and add in Figs.6b, c, d and compare to Fig.4a, we can recognize a factor $K(\underline{P}'; \underline{q}, \underline{q}')$ emerging for the "upper" loop. Finally,

$$S^{(2)} = -(4\pi e^4) \eta_P \delta(\eta_P - \eta_{P'}) \delta_{S'S} \int \frac{d\tilde{q}}{(2\pi)^2} \frac{d\tilde{q}'}{(2\pi)^2} \frac{d\tilde{q}''}{(2\pi)^2} \int \frac{d\alpha}{\alpha} \frac{d\gamma}{\gamma} \theta(1-\alpha) \theta(\alpha-\gamma)$$

$$\left[(\tilde{P}' - \tilde{q})^2 + \lambda^2 \right]^{-1} \left[(\tilde{P}' + \tilde{q})^2 + \lambda^2 \right]^{-1} \left[(\tilde{P}' - \tilde{q}')^2 + \lambda^2 \right]^{-1} \left[(\tilde{P}' + \tilde{q}')^2 + \lambda^2 \right]^{-1} \left[(\tilde{P}' - \tilde{q}'')^2 + \lambda^2 \right]^{-1} \left[(\tilde{P}' + \tilde{q}'')^2 + \lambda^2 \right]^{-1}$$

$$K(\tilde{P}'; \tilde{q}, \tilde{q}') K(\tilde{P}'; \tilde{q}', \tilde{q}'') \quad (\text{B.4})$$

The integrations over the η -fractions of the photons must be cutoff from below in the same way as done in the single loop diagram,

$$\int_{\frac{\eta_{\min}}{\eta_P}}^1 \frac{d\alpha}{\alpha} \int_{\frac{\eta_{\min}}{\eta_P}}^{\alpha} \frac{d\lambda}{\lambda} \cong \frac{1}{2!} \log^2 \left(\frac{\eta_P}{\eta_{\min}} \right) \quad (\text{B.5})$$

We have done enough analysis now to see that the scattering amplitude with $N e^+ e^-$ loops must be given by,

$$S^{(N)} = -(4\pi e^4) \eta_P \delta(\eta_P - \eta_{P'}) \delta_{S'S} \frac{1}{N!} \log^N \left(\frac{\eta_P}{\eta_{\min}} \right) I^{(N+1)}(\tilde{P}') \quad (\text{B.6})$$

where

$$I^{(N)}(\tilde{P}') = \int \frac{d\tilde{k}_1}{(2\pi)^2} \cdots \frac{d\tilde{k}_N}{(2\pi)^2} \frac{1}{\left[(\tilde{P}' - \tilde{k}_1)^2 + \lambda^2 \right] \left[(\tilde{P}' + \tilde{k}_1)^2 + \lambda^2 \right] \cdots \left[(\tilde{P}' - \tilde{k}_N)^2 + \lambda^2 \right] \left[(\tilde{P}' + \tilde{k}_N)^2 + \lambda^2 \right]}$$

$$K(\tilde{P}'; \tilde{k}_1, \tilde{k}_2) K(\tilde{P}'; \tilde{k}_2, \tilde{k}_3) \cdots K(\tilde{P}'; \tilde{k}_{N-1}, \tilde{k}_N) \quad (\text{B.7})$$

The crucial factors of $\log^N \eta_P$ and $N!$ arise as they did for the 2-loop diagram.

In particular, the amplitude receives a factor from the N strongly-ordered photons of,

$$\int^1 \frac{dx_1}{x_1} \int^{x_1} \frac{dx_2}{x_2} \cdots \int_{\frac{\eta_{\min}}{\eta_P}}^{x_{N-1}} \frac{dx_N}{x_N} \cong \frac{1}{N!} \log^N \left(\frac{\eta_P}{\eta_{\min}} \right) \quad (\text{B. 8})$$

In the next Appendix we will see that we can sum all the $S^{(N)}$ in the forward direction.

APPENDIX C. BRANCH CUT ($m=\lambda=0$)

We wish to study $S^{(N)}$ in the forward direction. For $\underline{P}'=\underline{P}=0$, we have

$$S^{(N)}(\underline{P}=0) = -(4\pi e^4) \eta_P \delta(\eta_P - \eta_{P'}) \frac{1}{N!} \log^N(\eta_P) I^{(N+1)}(\underline{P}=0) \quad (C.1)$$

where

$$I^{(N)}(0) = \int \frac{d\underline{k}_1}{(2\pi)^2} \cdots \frac{d\underline{k}_N}{(2\pi)^2} \frac{1}{(\underline{k}_1^2 + \lambda^2)^2 \cdots (\underline{k}_N^2 + \lambda^2)^2} K(\underline{k}_1, \underline{k}_2) K(\underline{k}_2, \underline{k}_3) \cdots K(\underline{k}_{N-1}, \underline{k}_N)$$

and we have defined,

$$K(\underline{k}_i, \underline{k}_{i+1}) \equiv K(\underline{P}'=0; \underline{k}_i, \underline{k}_{i+1})$$

We can solve for $I^{(N)}$ explicitly, and sum the amplitudes $S^{(N)}$ in the case $m=\lambda=0$. (However, λ must be held non-zero in the first and last propagators on the chain in order to avoid a spurious infra-red divergence.) We might argue, instead of setting $m=\lambda=0$, that we are integrating only over that part of phase space for which $\underline{k}^2 \gg m^2, \lambda^2$. In that case we will obtain here at least a lower bound on the "real" scattering amplitude.

Recall from Appendix B that when $m=0$,

$$K(\underline{k}_1, \underline{k}_2) = \left(\frac{8\alpha^2}{\pi} \right) \underline{k}_1^2 \underline{k}_2^2 B_0(\underline{k}_1, \underline{k}_2) \quad (C.2)$$

where

$$B(\underline{k}_1, \underline{k}_2) = \int_0^1 dx \int_0^1 dy \frac{x(1-x)+y(1-y)-5x(1-x)y(1-y)}{x(1-x)\underline{k}_1^2 + y(1-y)\underline{k}_2^2}$$

and we have averaged over the free angle $\underline{k}_1 \cdot \underline{k}_2$ already. Substituting this

into (C. 1), we have,

$$I^{(N)} = \left(\frac{8\alpha^2}{\pi} \right)^{N-1} \frac{1}{(2\pi)^{2N}} \int d\tilde{k}_1 d\tilde{k}_N \frac{\tilde{k}_1^2}{(\tilde{k}_1^2 + \lambda^2)^2} \frac{\tilde{k}_N^2}{(\tilde{k}_N^2 + \lambda^2)^2} B(\tilde{k}_1, \tilde{k}_2) B(\tilde{k}_2, \tilde{k}_3) \dots B(\tilde{k}_{N-1}, \tilde{k}_N) \cdot \\ d\tilde{k}_2 \dots d\tilde{k}_{N-1} \quad (C. 3)$$

It will prove convenient to scale the (momentum)⁻² dimension out of B. To do this we change variables,

$$|\tilde{k}_1| = \kappa e^{\xi_1}, \dots, |\tilde{k}_N| = \kappa e^{\xi_N}$$

and note that,

$$B(\kappa e^{\xi_1}, \kappa e^{\xi_2}) = \kappa^{-2} B(e^{\xi_1}, e^{\xi_2})$$

then,

$$I^{(N)} = \left(\frac{8\alpha^2}{\pi} \right)^{N-1} \frac{1}{(2\pi)^N} \frac{1}{\kappa^2} \int d\xi_1 d\xi_N \frac{e^{4(\xi_1 + \xi_N)}}{\left(e^{2\xi_1 + \frac{\lambda^2}{\kappa^2}} \right)^2 \left(e^{2\xi_N + \frac{\lambda^2}{\kappa^2}} \right)^2} \\ e^{2(\xi_2 + \xi_3 + \dots + \xi_{N-1})} B(e^{\xi_1}, e^{\xi_2}) B(e^{\xi_2}, e^{\xi_3}) \dots B(e^{\xi_{N-1}}, e^{\xi_N}) \quad (C. 4)$$

Notice that,

$$e^{(\xi_1 + \xi_2)} B(e^{\xi_1}, e^{\xi_2}) = \int dx dy \frac{x(1-x) + y(1-y) - 5x(1-x)y(1-y)}{x(1-x) \exp\left[+(\xi_1 - \xi_2)\right] + y(1-y) \exp\left[-(\xi_1 - \xi_2)\right]} \equiv C(\xi_1 - \xi_2)$$

is a function only of the difference $(\xi_1 - \xi_2)$. We should, therefore, change integration variables,

$$\eta_1 = \xi_1, \quad \eta_2 = \xi_1 - \xi_2, \quad \eta_3 = \xi_2 - \xi_3, \dots, \quad \eta_{N-1} = \xi_{N-2} - \xi_{N-1}, \quad \eta_N = \xi_N$$

So,

$$I^{(N)} = \left(\frac{8\alpha^2}{\pi} \right)^{N-1} \frac{1}{(2\pi)^N} \frac{1}{\kappa^2} \int d\eta_1 \dots d\eta_N \frac{e^{3(\eta_1 + \eta_N)}}{\left(e^{2\eta_1 + \frac{\lambda^2}{\kappa^2}} \right)^2 \left(e^{2\eta_N + \frac{\lambda^2}{\kappa^2}} \right)^2} \cdot \quad (C.5)$$

$$C(\eta_2)C(\eta_3)\dots C(\eta_{N-1})C(\eta_1 - \eta_2 - \eta_3 - \dots - \eta_N)$$

The resulting convolution integral is factored upon introducing Fourier transforms,

$$C(\eta) \equiv \int \frac{d\beta}{(2\pi)} e^{i\eta\beta} \tilde{C}_0(\beta)$$

Then,

$$I^{(N)} = \left(\frac{8\alpha^2}{\pi} \right)^{N-1} \frac{1}{(2\pi)^N \kappa^2} \int \frac{d\beta}{(2\pi)} e^{i(\eta_1 - \eta_N)\beta} \frac{e^{3(\eta_1 + \eta_N)}}{\left(e^{2\eta_1 + \frac{\lambda^2}{\kappa^2}} \right)^2 \left(e^{2\eta_N + \frac{\lambda^2}{\kappa^2}} \right)^2} \left[\tilde{C}(\beta) \right]^{N-1} d\eta_1 d\eta_N \quad (C.6)$$

Introducing the function

$$f(\beta, \gamma) = \int d\eta e^{-i\eta\beta} \frac{e^{3\eta}}{(e^{2\eta + \gamma^2})^2} \quad (C.7)$$

We can write finally,

$$I^{(N)} = \left(\frac{8\alpha^2}{\pi} \right)^{N-1} \frac{1}{(2\pi)^N \kappa^2} \int \frac{d\beta}{(2\pi)} f^*(\beta, \frac{\lambda}{\kappa}) f(\beta, \frac{\lambda}{\kappa}) \left[\tilde{C}(\beta) \right]^{N-1} \quad (C.8)$$

The properties of the functions f and C are derived in Appendix D. From (D.4, 6, 10), we have

$$f(\beta, \gamma) = \gamma^{-(1+i\beta)} f(\beta, 1)$$

$$f(\beta, 1) = \frac{1}{2} \Gamma\left(\frac{1}{2} + \frac{i\beta}{2}\right) \Gamma\left(\frac{3}{2} - \frac{i\beta}{2}\right) = \frac{1}{2} B\left(\frac{1}{2} + \frac{i\alpha}{2}, \frac{3}{2} - \frac{i\alpha}{2}\right)$$

$$\tilde{C}(0) = \frac{11\pi^3}{2^7}, \quad \tilde{C}'(0) = 0, \quad \tilde{C}''(0) = -\frac{11\pi^3}{32} \left(\frac{\pi^2}{12} - \frac{1}{44} \right) \quad (\text{C.9})$$

Having calculated $I^{(N)}$ we can return to the scattering amplitude and note that $\sum_{N=1}^{\infty} S^{(N)}$ is just an exponential series,

$$S^{(1 \text{ chain})} \equiv \sum_{N=1}^{\infty} S^{(N)} = -(4\pi e^4) \eta_P \delta(\eta_P - \eta_{P'}) \left[\frac{1}{\lambda^2} \int \frac{d\beta}{(2\pi)^2} f^*(\beta, 1) f(\beta, 1) \cdot \right. \\ \left. e^{\left(\frac{2\alpha}{\pi}\right)^2 \tilde{C}(\beta) \log \eta_{P-1}} \right] \quad (\text{C.10})$$

If we imagine letting $\eta \rightarrow \infty$, we can evaluate the leading part of the integral straightforwardly,

$$S^{(1 \text{ chain})} \cong -(4\pi e^4) \eta_P \delta(\eta_P - \eta_{P'}) e^{\left(\frac{2\alpha}{\pi}\right)^2 \tilde{C}(0) \log \eta_P} \int \frac{d\beta}{(2\pi)^2} f^*(\beta, 1) f(\beta, 1) \cdot \\ e^{\left(\frac{2\alpha}{\pi}\right)^2 [\tilde{C}(\beta) - \tilde{C}(0)] \log \eta_P} \quad (\text{C.11})$$

$$S^{(1 \text{ chain})} \approx -(4\pi e^4) \eta_P \delta(\eta_P - \eta_{P'}) e^{\left(\frac{2\alpha}{\pi}\right)^2 \tilde{C}(0) \log \eta_P} .$$

$$\frac{f^*(0, 1) f(0, 1)}{(2\pi)^2 \lambda^2} \int d\beta e^{-\frac{1}{2} \left(\frac{2\alpha}{\pi}\right)^2 \left| \tilde{C}''(0) \right| \log \eta_P} \cdot \beta^2$$

$$S^{(1 \text{ chain})} \approx -(4\pi e^4) \frac{|f(0, 1)|^2}{(2\pi)^2 \lambda^2} \left(\frac{2\pi}{\left| \left(\frac{2\alpha}{\pi}\right)^2 \tilde{C}''(0) \right|} \right)^{\frac{1}{2}} \delta(\eta_P - \eta_{P'}) \frac{(\eta_P)^{1 + \left(\frac{2\alpha}{\pi}\right)^2 \tilde{C}(0)}}{\sqrt{\log \eta_P}} \quad (\text{C. 12})$$

The factor $\log^{-\frac{1}{2}} \eta_P$ is indicative of the square root character of the branch cut responsible for $S^{(1 \text{ chain})}$. We see also that the branch cut extends to $J = 1 + \left(\frac{2\alpha}{\pi}\right)^2 \tilde{C}(0) = 1 + \frac{11\pi}{32} \alpha^2$, which shows that the single chain multiperipheral diagrams summed alone violate the Froissart bound.

In preparation for a subsequent discussion, consider in more detail the structure of this cut singularity in the J -plane. Rewrite (C. 10),

$$S^{(1 \text{ chain})} = -(2\pi)(2\eta_P) \delta(\eta_P - \eta_{P'}) \left[M\left(\frac{\eta_P}{\eta_{\min}}\right) - 1 \right] \quad (\text{C. 13})$$

where

$$M\left(\frac{\eta_P}{\eta_{\min}}\right) = \frac{1}{\lambda^2} \int \frac{d\beta}{(2\pi)^2} f^*(\beta, 1) f(\beta, 1) \left(\frac{\eta_P}{\eta_{\min}}\right)^{\left(\frac{2\alpha}{\pi}\right)^2 \tilde{C}(\beta)} \theta\left(\frac{\eta_P}{\eta_{\min}} - 1\right) \quad (\text{C. 14})$$

The θ -function simply states the trivial fact that the S-matrix is different from unity only when $\eta_{\mathbf{P}} > \eta_{\min}$. To discuss the behavior of the scattering amplitude from the complex angular momentum point of view, we turn to the Mellin transform of $M(J)$. We easily compute from (C.13) that

$$M(J) = \frac{1}{\lambda^2} \int \frac{d\beta}{(2\pi)^2} f^*(\beta, 1) f(\beta, 1) \left[\frac{1}{J - \left(\frac{2\alpha}{\pi}\right)^2 \tilde{C}(\beta)} \right] \quad (\text{C.15})$$

Therefore, $M(J)$ possesses a cut over that range of J for which there is a solution to the equation

$$J = \left(\frac{2\alpha}{\pi}\right)^2 \tilde{C}(\beta) \quad (\text{C.16})$$

We recall from Appendix D that $\tilde{C}(\beta)$ is an even, positive function with a maximum at $\beta=0$, and decreases monotonically to zero as β increases. Therefore, the cut extends from $J_{\min}=0$ to $J_{\max} = \left(\frac{2\alpha}{\pi}\right)^2 \tilde{C}(0) = \frac{11\pi}{32} \alpha^2$.

The discontinuity of $M(J)$ across the cut is,

$$\text{Disc } M(J) = -\frac{\pi}{\lambda^2} \int \frac{d\beta}{(2\pi)^2} f^*(\beta, 1) f(\beta, 1) \delta \left[J - \left(\frac{2\alpha}{\pi}\right)^2 \tilde{C}(\beta) \right] \quad (\text{C.17})$$

Since the high energy behavior of the scattering amplitude is controlled by the behavior of $\text{Disc } M(J)$ near J_{\max} , we shall obtain the right hand side of (C.17) explicitly in this region. To do this it suffices to solve (C.16) for β in terms of J near the endpoint $\beta=0$. (C.16) reads, to second order in β ,

$$J = \left(\frac{2\alpha}{\pi}\right)^2 \left[\tilde{C}(0) + \frac{1}{2} \tilde{C}''(0) \beta^2 \right]$$

So,

$$\beta = \sqrt{\frac{J_{\max} - J}{D}}$$

where

$$D = -\frac{1}{2} \left(\frac{2\alpha}{\pi}\right)^2 \tilde{C}''(0) = \frac{11\pi}{16} \left(\frac{\pi^2}{12} - \frac{1}{44} \right) \alpha^2$$

Finally, for J less than but near J_{\max} ,

$$\text{Disc } M(J) \cong -\frac{\pi}{\lambda^2} \int \frac{d\beta}{(2\pi)^2} f^*(\beta, 1) f(\beta, 1) \frac{\delta\left(\beta - \sqrt{\frac{J_{\max} - J}{D}}\right)}{2\sqrt{D(J_{\max} - J)}}$$

$$\text{Disc } M(J) \cong \left[\frac{\pi}{2^7 \lambda^2 \sqrt{D}} \right] \frac{1}{\sqrt{J_{\max} - J}} \quad (\text{C. 18})$$

where we have substituted the numerical value $f(0, 1) = \frac{\pi}{4}$. (C. 18) shows the square root character of the cut. Furthermore, it is easy to take (C. 18) and invert the Mellin transform

$$M(y) = \frac{1}{\pi} \int_0^{J_{\max}} y^J \text{Disc } M(J) dJ$$

and rederive (C. 12).

APPENDIX D PROPERTIES OF f AND C

In order to complete the discussion of the branch cut we should simplify the functions

$$f(\alpha, \beta) = \int_{-\infty}^{\infty} d\eta e^{-i\eta\alpha} \frac{e^{3\eta}}{(e^{2\eta} + \beta^2)^2} \quad (D. 1)$$

$$C(\xi) = \int dx dy \frac{x(1-x)+y(1-y)-5x(1-x)y(1-y)}{x(1-x)e^{+\xi} + y(1-y)e^{-\xi}} \quad (D. 2)$$

which were introduced in Appendix C.

Consider the function $f(\alpha, \beta)$ first. It is easy to see that the function's dependence on β can be scaled out. If we define a new integration variable y ,

$$\frac{1}{\beta} e^{\eta} = y$$

we can rewrite (D. 1) as,

$$f(\alpha, \beta) = \beta^{-(1+i\alpha)} f(\alpha, 1)$$

$$f(\alpha, 1) = \int_0^{\infty} dy \frac{y^{2-i\alpha}}{(y^2+1)^2}$$

Furthermore, $f(\alpha, 1)$ can be identified as Beta function if we change variables in the integrand to,

$$u = \frac{1}{y^2+1}$$

then,

$$f(\alpha, 1) = \frac{1}{2} \int_0^1 du u^{-\frac{1}{2} + \frac{i\alpha}{2}} (1-u)^{\frac{1}{2} - \frac{i\alpha}{2}}$$

which is just,

$$f(\alpha, 1) = \frac{1}{2}B\left(\frac{1}{2} + \frac{i\alpha}{2}, \frac{3}{2} - \frac{i\alpha}{2}\right) = \Gamma\left(\frac{1}{2} + \frac{i\alpha}{2}\right) \Gamma\left(\frac{3}{2} - \frac{i\alpha}{2}\right) \quad (D. 3)$$

Our determination of the character of the branch cut relied upon the nonvanishing of $f(0, 1)$. In fact,

$$f(0, 1) = \Gamma\left(\frac{1}{2}\right) \Gamma\left(\frac{3}{2}\right) = \frac{\pi}{4} \quad (D. 5)$$

Now we turn to the function $C(\xi)$. We wish to compute its Fourier transform,

$$\tilde{C}(\beta) = \int d\xi e^{-i\beta\xi} C(\xi) \quad (D. 6)$$

Using the transform,

$$\int d\xi e^{-i\beta\xi} \left(\frac{1}{x(1-x)e^{\xi} + y(1-y)e^{-\xi}} \right) = \frac{\pi}{2 \cosh\left(\frac{\pi}{2}\beta\right)} \left[x(1-x) \right]^{-\frac{1}{2} + i\frac{\beta}{2}} \left[y(1-y) \right]^{-\frac{1}{2} - i\frac{\beta}{2}} \quad (D. 7)$$

we have,

$$\tilde{C}(\beta) = \frac{\pi}{2 \cosh\left(\frac{\pi}{2}\beta\right)} \int dx dy \left\{ \left[x(1-x) \right]^{\frac{1}{2} + i\frac{\beta}{2}} \left[y(1-y) \right]^{-\frac{1}{2} - i\frac{\beta}{2}} + \left[x(1-x) \right]^{-\frac{1}{2} + i\frac{\beta}{2}} \left[y(1-y) \right]^{-\frac{1}{2} - i\frac{\beta}{2}} - 5 \left[x(1-x) \right]^{\frac{1}{2} + i\frac{\beta}{2}} \left[y(1-y) \right]^{\frac{1}{2} - i\frac{\beta}{2}} \right\} \quad (D. 8)$$

which we recognize as the sum of products of Beta functions. So,

$$\tilde{C}(\beta) = \frac{\pi}{2 \cosh(\frac{\pi}{2}\beta)} \left\{ \frac{\left[\Gamma(\frac{3}{2} + i\frac{\beta}{2}) \right]^2 \left[\Gamma(\frac{1}{2} - i\frac{\beta}{2}) \right]^2}{\Gamma(3+i\beta) \Gamma(1-i\beta)} + \frac{\left[\Gamma(\frac{3}{2} - i\frac{\beta}{2}) \right]^2 \left[\Gamma(\frac{1}{2} + i\frac{\beta}{2}) \right]^2}{\Gamma(3-i\beta) \Gamma(1+i\beta)} \right. \\ \left. -5 \frac{\left[\Gamma(\frac{3}{2} + i\frac{\beta}{2}) \right]^2 \left[\Gamma(\frac{3}{2} - i\frac{\beta}{2}) \right]^2}{\Gamma(3+i\beta) \Gamma(3-i\beta)} \right\} \quad (D.9)$$

Furthermore, if we use various gamma function identities such as the "Reflection formula", (D.9) can be written in the final form,

$$\tilde{C}(\beta) = \frac{\pi^2}{16\beta} \left(\frac{11+3\beta^2}{4+\beta^2} \right) \frac{\sinh(\frac{\pi}{2}\beta)}{\cosh^2(\frac{\pi}{2}\beta)} \quad (D.10)$$

FOOTNOTES

1. H. Cheng and T. T. Wu, Phys. Rev. Letters 24, 1456 (1970).
2. J. B. Kogut and D. E. Soper, Phys. Rev D1, 2901 (1970), hereafter referred to as I.
J. D. Bjorken, J. B. Kogut and D. E. Soper, Phys. Rev D3, 1382 (1971), hereafter referred to as II.
3. R. P. Feynman, in Proceedings of the Third International Conference on High-Energy Collisions, Stony Brook, New York, 1969 (Gordon and Breach, New York, 1969) ; Phys. Rev. Letters 23, 1415 (1969).
4. H. Cheng and T. T. Wu, Phys.Rev. 186, 1611 (1969), Phys. Rev. D1, 2775 (1970).
5. G. V. Frolov, V. N. Gribov and L. N. Lipatov, Physics Letters 31B, 34 (1970).
6. A somewhat simpler proof can be given by appealing to Feynman diagrams instead of the old fashioned diagrams considered here (cf. S. J. Chang and P. M. Fishbane, Phys. Rev. D2, 1104 (1970)). However, in so doing one loses the space-time picture which will prove important later in the paper.
7. S. J. Chang and T. M. Yan, Phys. Rev. Letters 25, 1586 (1970)
Unfortunately the model considered in this paper is not indicative of the true behavior of $\lambda\phi^3$ field theory (cf. references in fn. 10). In fact, the single ladder graph of structureless, spin zero mesons violates the Froissart bound only when the coupling λ is large. Then the leading logarithm technique becomes unreliable. Nevertheless, some features

of these author's calculation (such as the strong absorption which saturates the Froissart bound) should survive a better treatment of the problem, and so we discuss their result briefly. Other workers have independently considered this model in considerable detail (cf. B. Hasslacher, D. K. Sinclair, G. M. Cicuta, and R. L. Sugar, Phys. Rev Letters 25, 1591 (1970)).

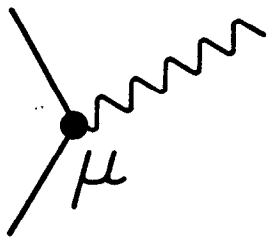
8. F. Smithies, Integral Equations (Cambridge University Press, Cambridge, 1962).
9. P. V. Landshoff and J. C. Polkinghorne, Phys. Rev. 181, 1989 (1969).
10. I. J. Muzinich, G. Tiktopoulos and S. B. Treiman, Phys. Rev. D3, 1041 (1971).

H. Cheng and T. T. Wu, D.E.S.Y. preprints Dec. and March.

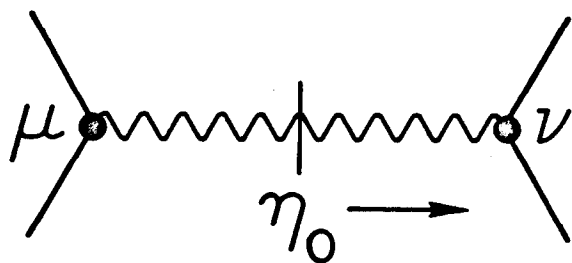
FIGURE CAPTIONS

1. Electrodynamic vertices at infinite momentum.
2. Dominant single loop diagrams.
3. One single loop diagram to represent the sum of diagrams in Fig. 2.
4. Single loop diagrams which a. contribute a leading logarithm, and b. do not contribute a leading logarithm.
5. Convenient kinematics for the single loop graph.
6. Double loop graphs.
7. Single chain graph.
8. Simplest double chain graph.
9. Simplest double chain graph contributing to the physical electron state.
Numbers 1-4 label the vertices.
10. Double chain graph.
11. The class of double chain graphs.
12. Simplest 2 chain-1 chain interference diagram.
13. The class of 2 chain-1 chain interference diagrams.
14. A simplified visualization of a 2 chain-1 chain interference diagram. The labels 1-4 denote the photon legs. In passing from Fig. 13 to this diagram we have untangled various photons for visual clarity.
15. Diagrammatic definition of the Reggeon appearing in Fig. 14.
16. A visualization of the function W and the integral equation it satisfies.
17. Iterations of Mandelstam cut diagrams.
18. A type of diagram with possible relevance to diffraction scattering.

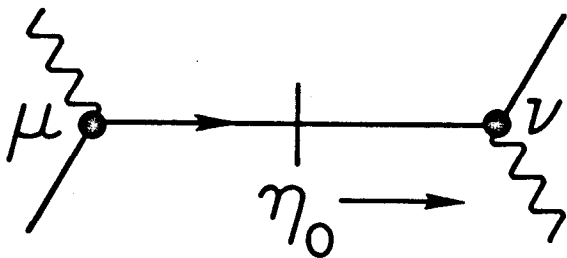
(a)



(b)

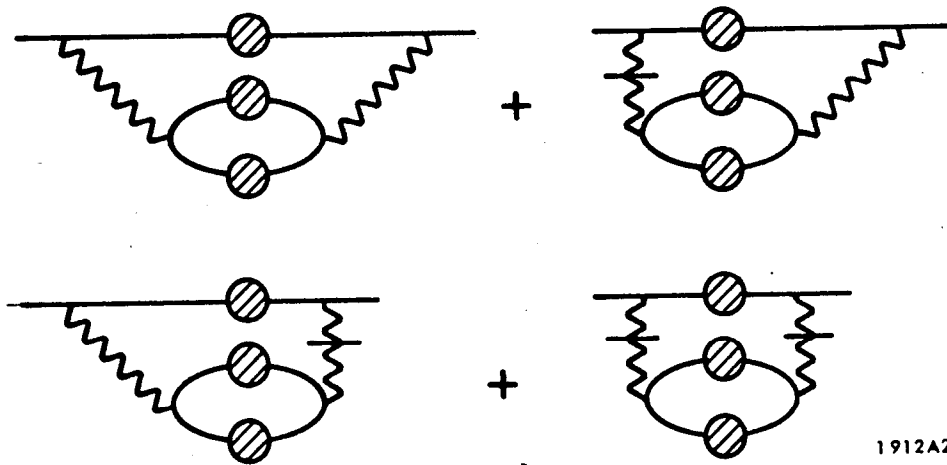


(c)



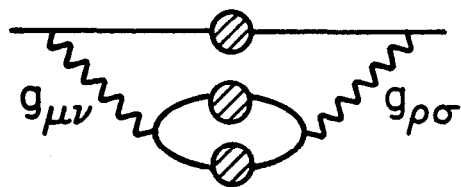
1463A5

Fig. 1



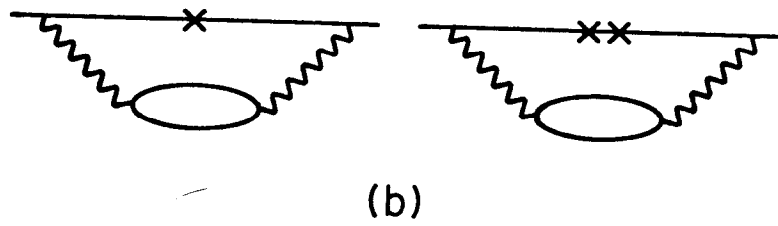
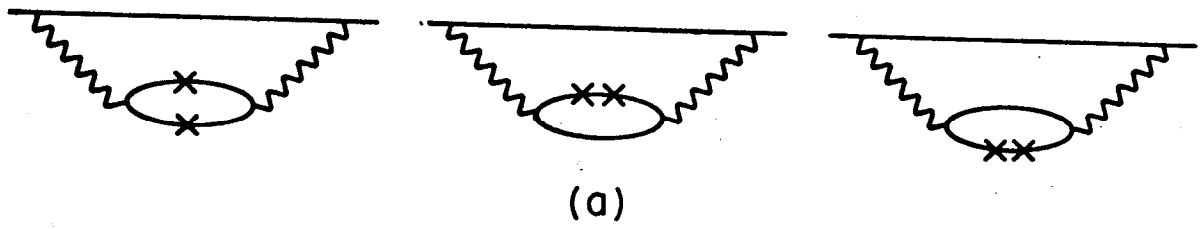
1912A2

Fig. 2



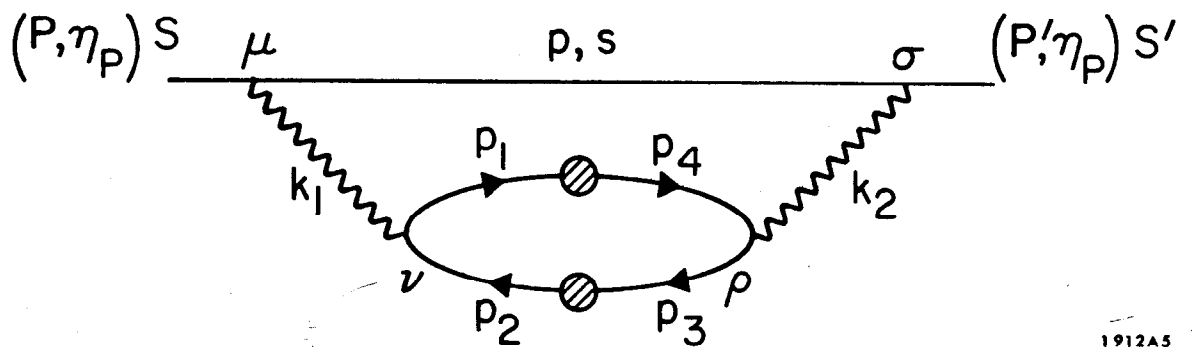
1912A3

Fig. 3



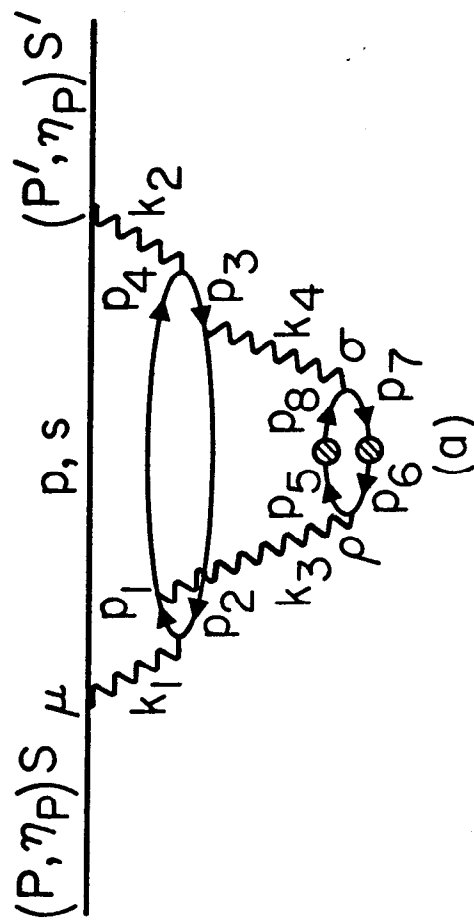
1912A4

Fig. 4

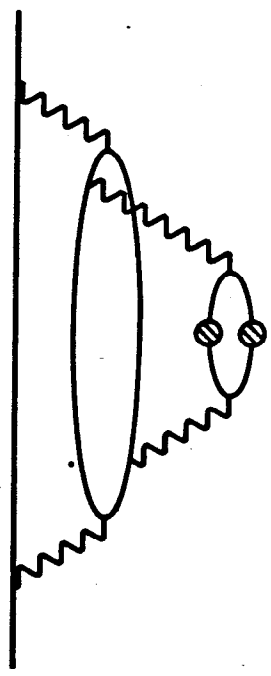


1912A5

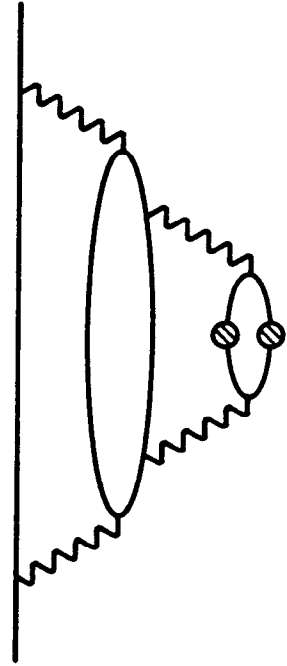
Fig. 5



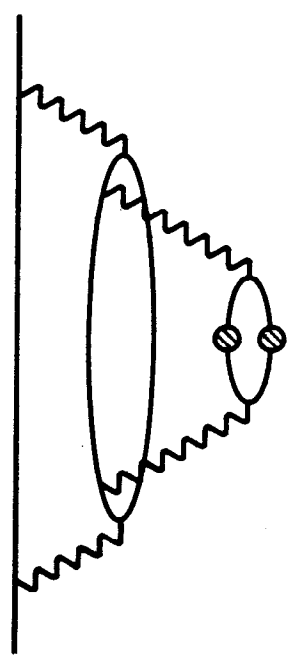
(a)



(b)

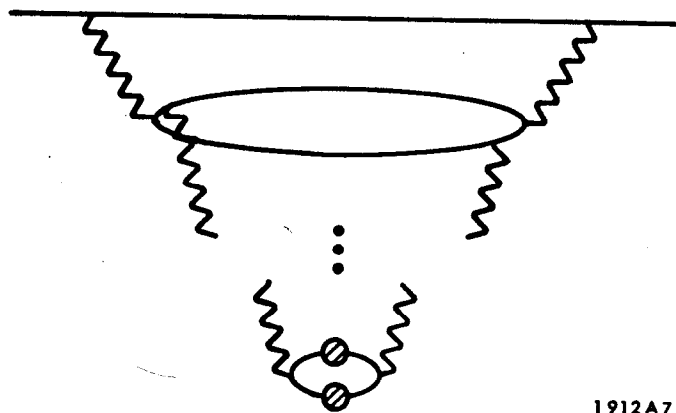


(c)



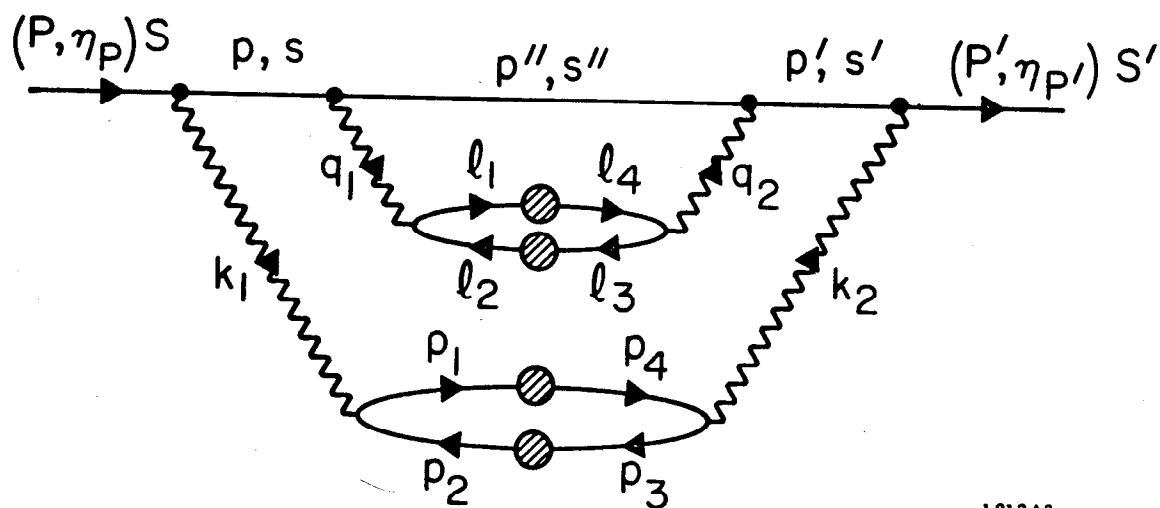
(d)

Fig. 6



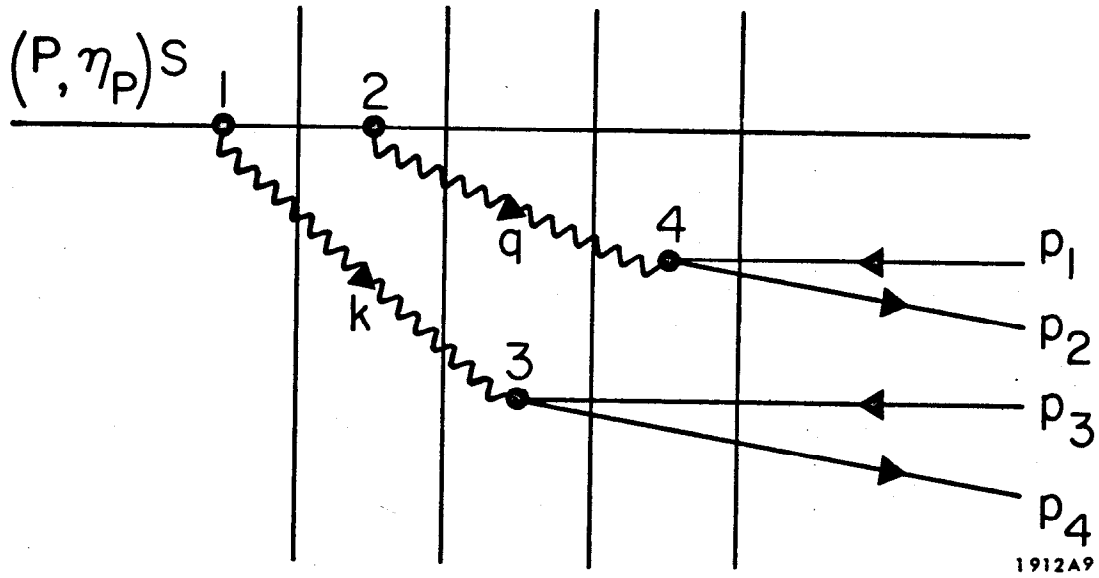
1912A7

Fig. 7



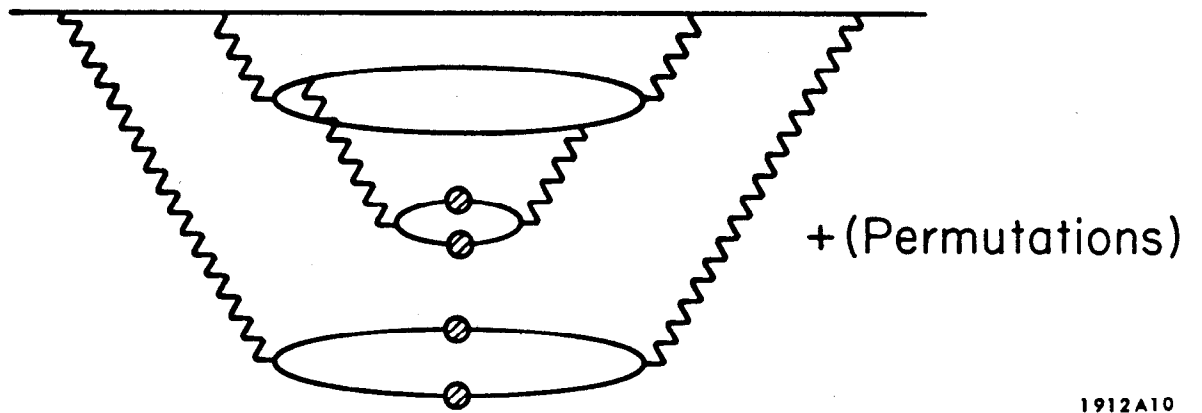
1912A8

Fig. 8



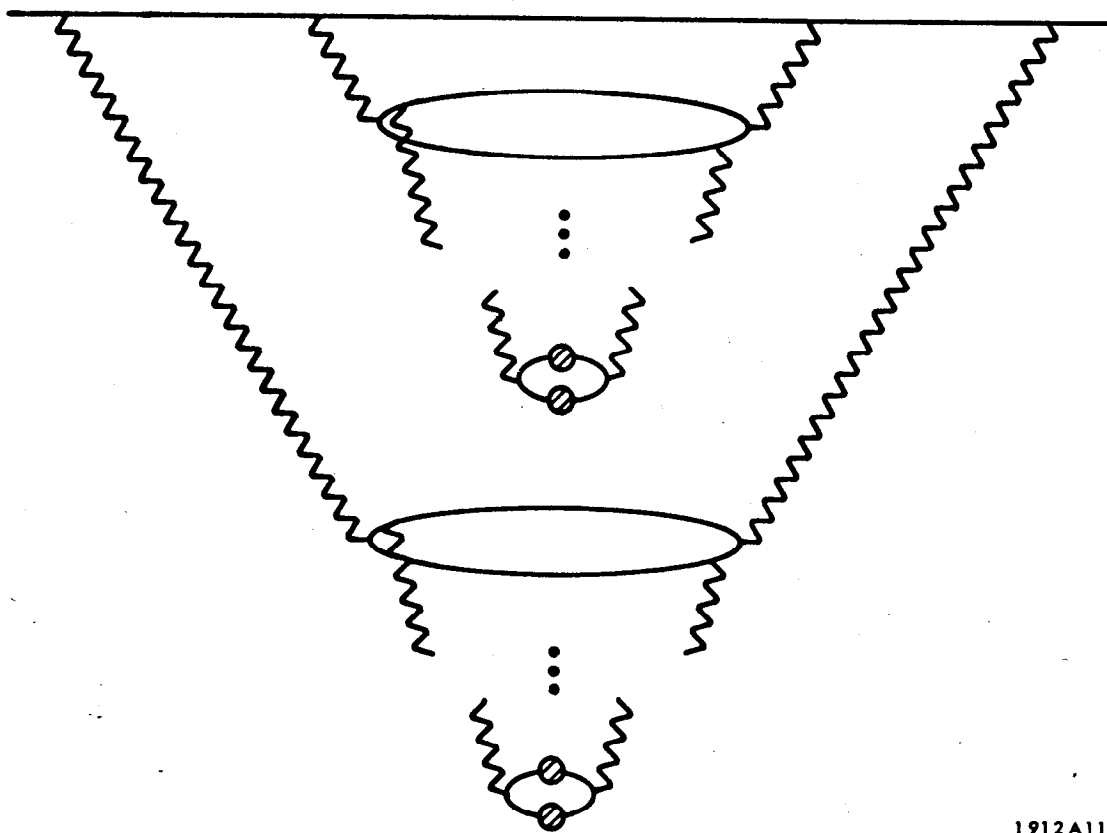
1912A9

Fig. 9



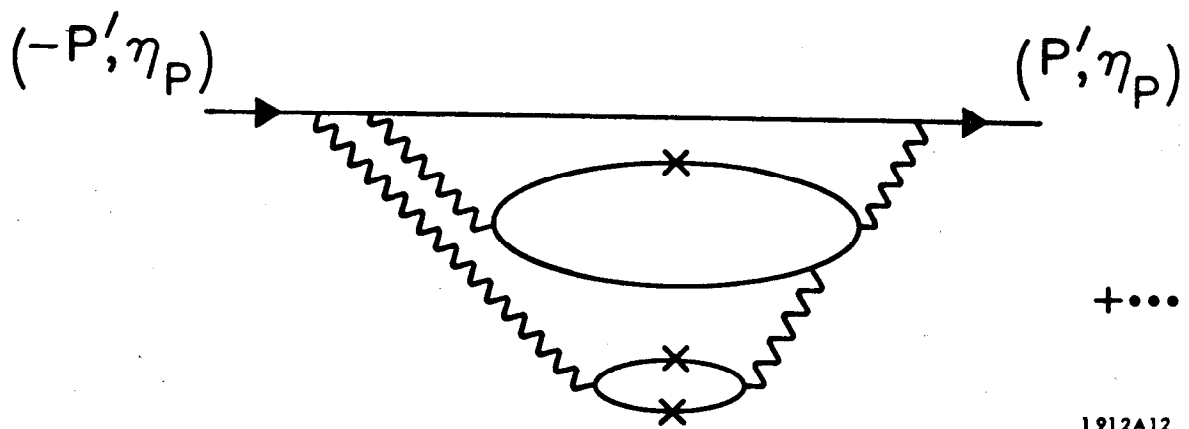
1912A10

Fig. 10



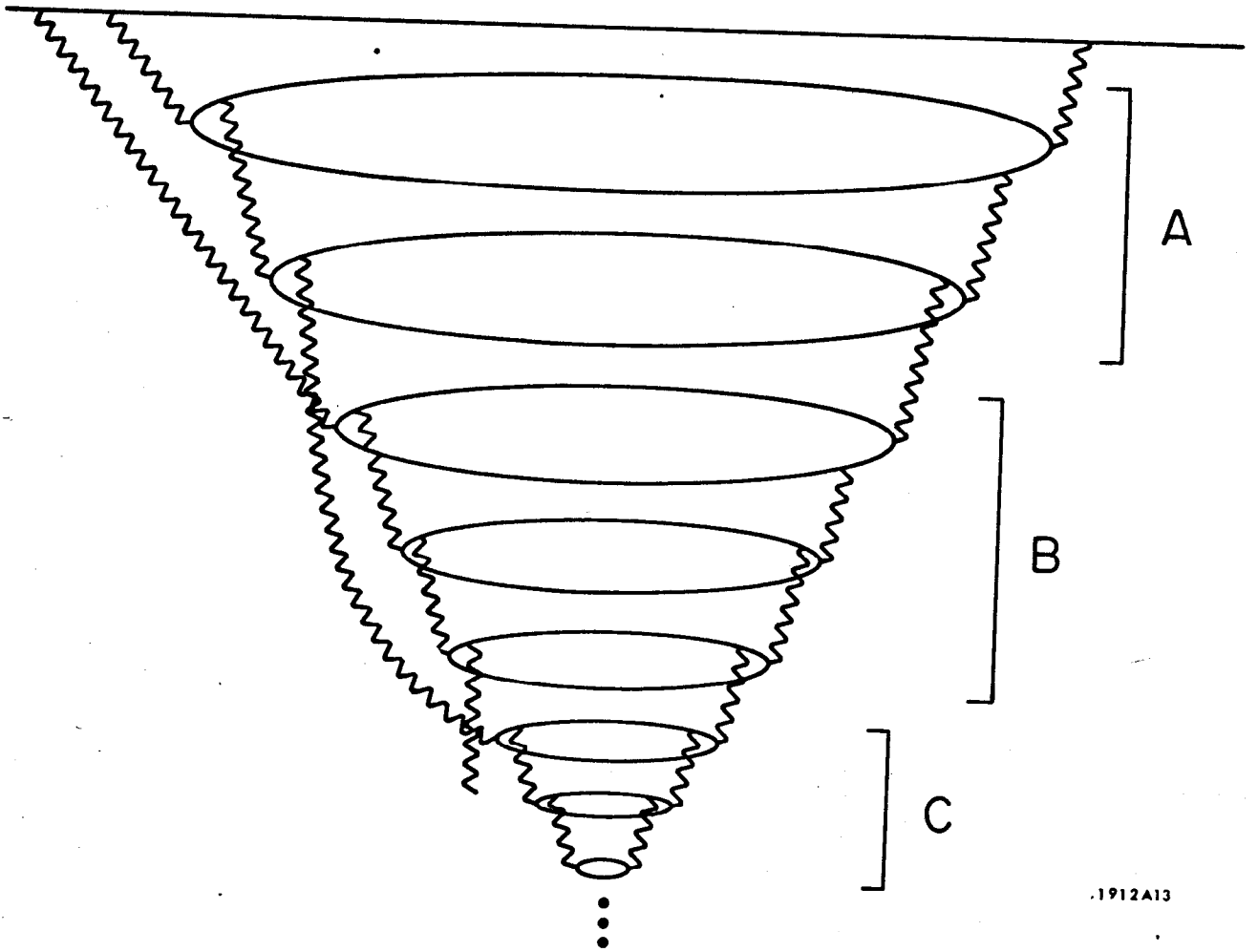
1912A11

Fig. 11



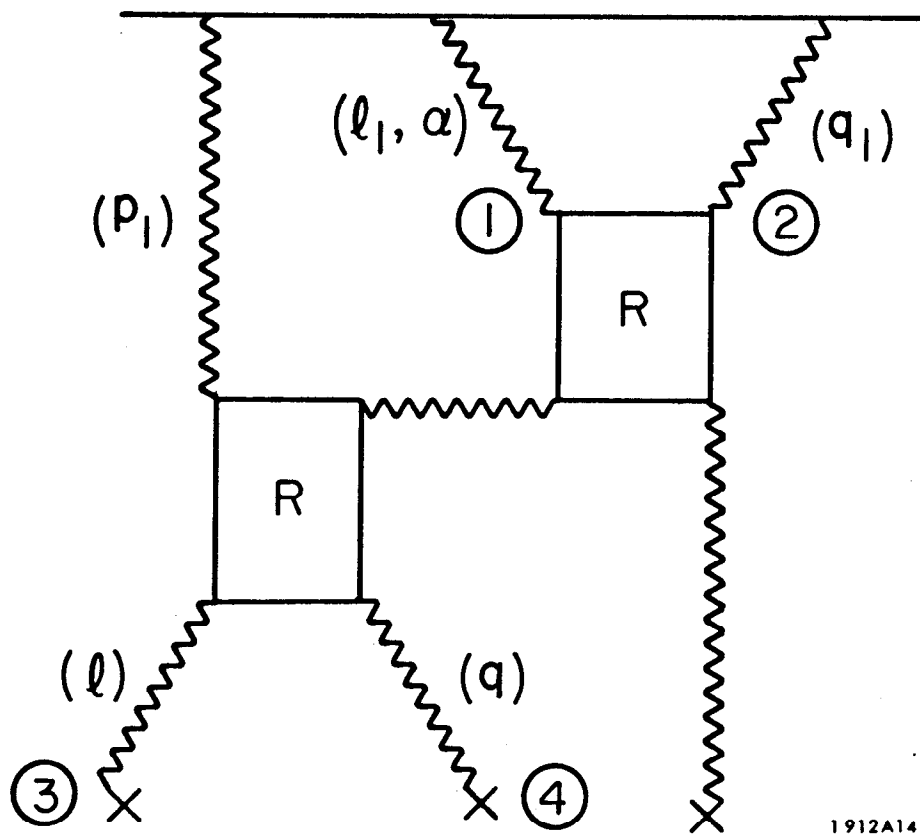
1912A12

Fig. 12



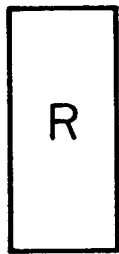
.1912A13

Fig. 13

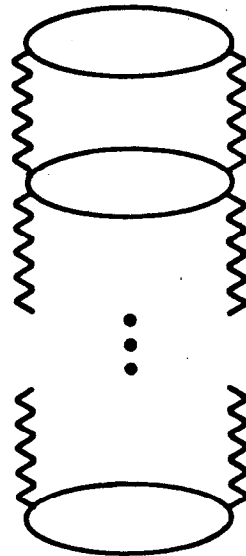


1912A14

Fig. 14

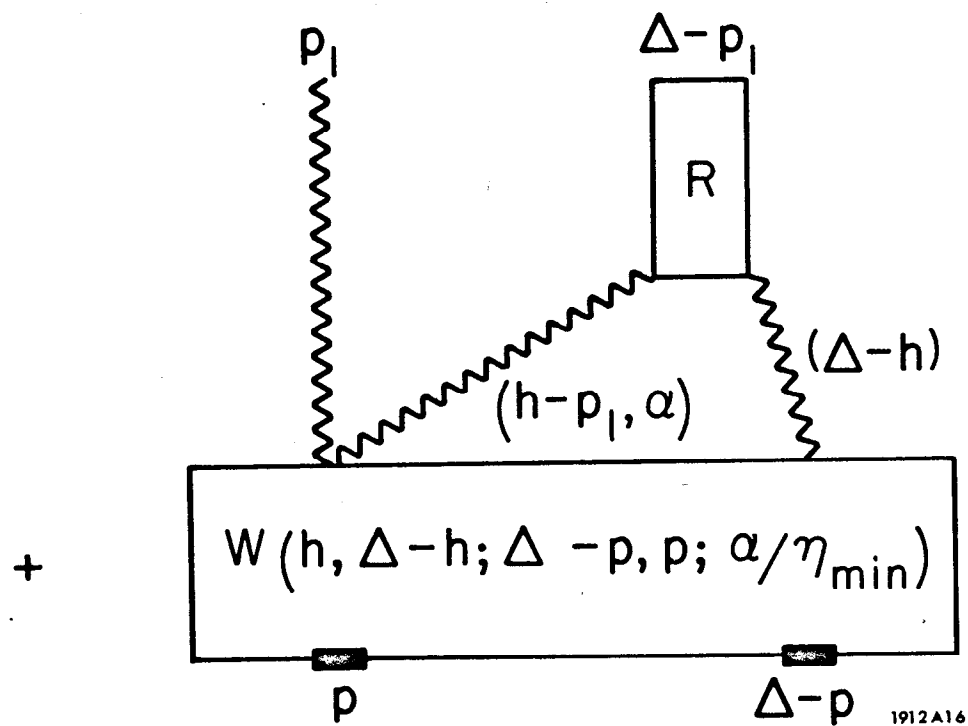
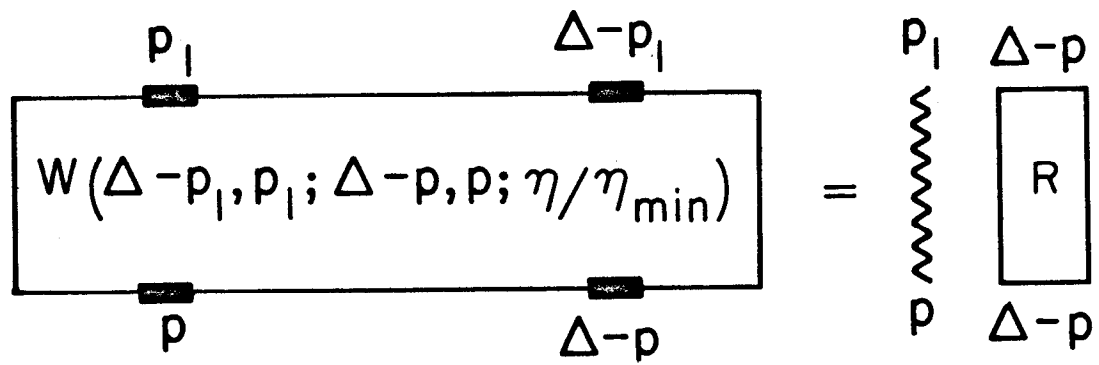


≡



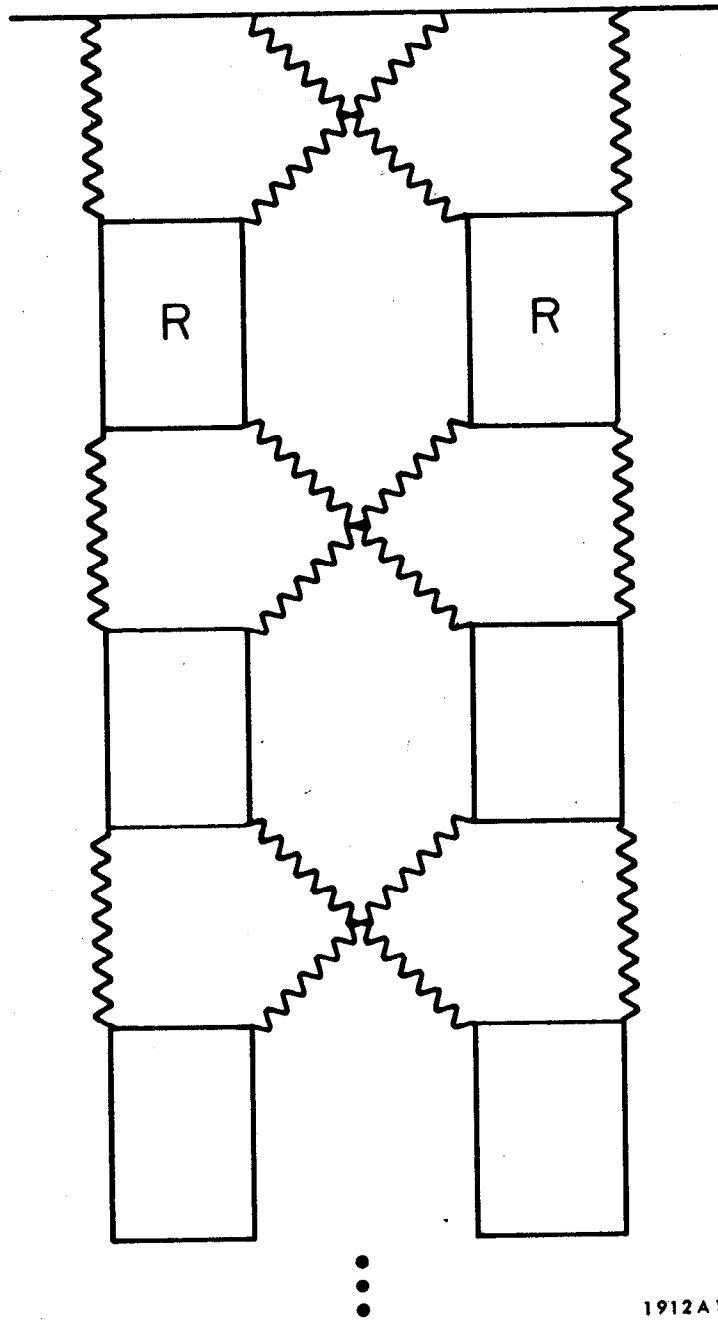
1912A15

Fig. 15



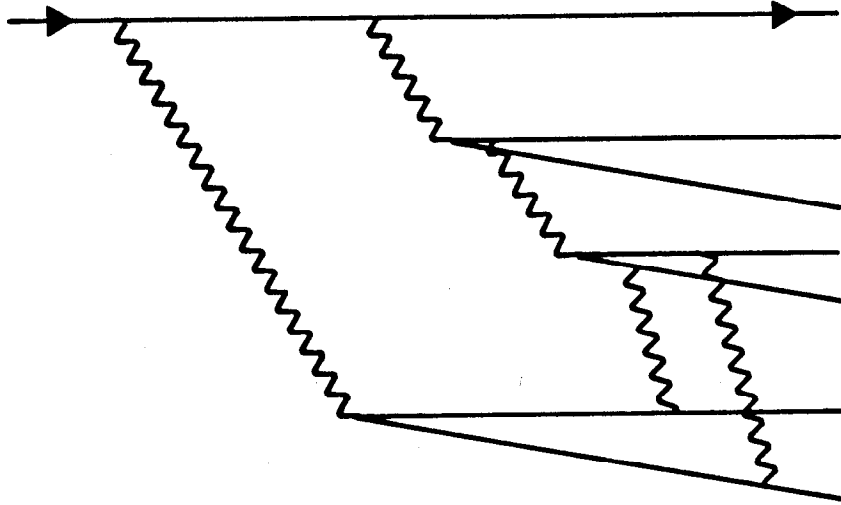
1912A16

Fig. 16



1912A17

Fig. 17



1912A18

Fig. 18